IOSR Journal of Applied Geology and Geophysics (IOSR-JAGG)
e-ISSN: 2321–0990, p-ISSN: 2321–0982.Volume 8, Issue 2 Ser. III (Mar – Apr 2020), PP 12-36
www.iosrjournals.org

Auriferous, uraniferous and REEs mineralized marl of Middle Um Bogma Formation, Southwestern Sinai, Egypt

Abd Elhadi A. Abbas
Nuclear Materials Authority, P.O. Box – 530 Maadi, Cairo, Egypt.

Abstract: Um Bogma Formation is considered the most important Formation in the Um Bogma area due to its content from uranium, Mn-Fe ore deposits and copper mineralization. The middle member of Um Bogma Formation consists mainly of marl and clay with some intercalated shale. The eU/eTh values of the investigated marl suggesting that these rocks are considered as productive uraniferous rocks and sites of deposition, especially at Talet Seliem and Allouga. Talet Seliem, Abu Thour, Allouga and Abu Zarab localities clarified that the mineral association are mainly represented by autonite, cerianite, pyrite, corandite, iron oxides and clays-bearing REEs and bastanesite in Talet Seliem, REEs mainly Nd adsorbed on clay and gypsum, aurorite and monazite in Abu Thour, brannerite, uraninite, carnotite and torbernite in Allouga and thorite, paratacamite, malachite, galena and jarosite in Abu Zarab, also gold is present in the four localities. The marl of Talet Seliem, Abu Thour, Allouga and Abu Zarab localities is highly enriched in Ag, Au, U and REEs, in addition to Zn, Cu and Pb. Gold and silver are present in the four localities with anomalous contents reaches 1.78 and 27.15 ppm respectively. It can be concluded that U and REEs were likely leached from the upper acidic environments (Talet Seliem, Abu Thor and Abu Zarab) and concentrated in the lower alkalic zone under reducing conditions (Allouga) as indicated from geomorphological studies.

Key wards: gold; uranium; base metals; rare earth elements

Date of Submission: 13-04-2020 Date of Acceptance: 28-04-2020

-

I. Introduction

The study area which is located between lat. 28º 55` – 29º 05` N and long. 33º 20` - 33º 25` E(Fig. 1) is considered a part of east Abu Zeneima promising area. This promising area covered mainly by the Paleozoic sediments which have importance owing to its content from economic ores as cool, copper, manganese, kaolin, glass sands, REEs and uranium. It reveals moderate to low topography and covered in part by Precambrian rocks which are overlain uonconformably by Paleozoic succession.

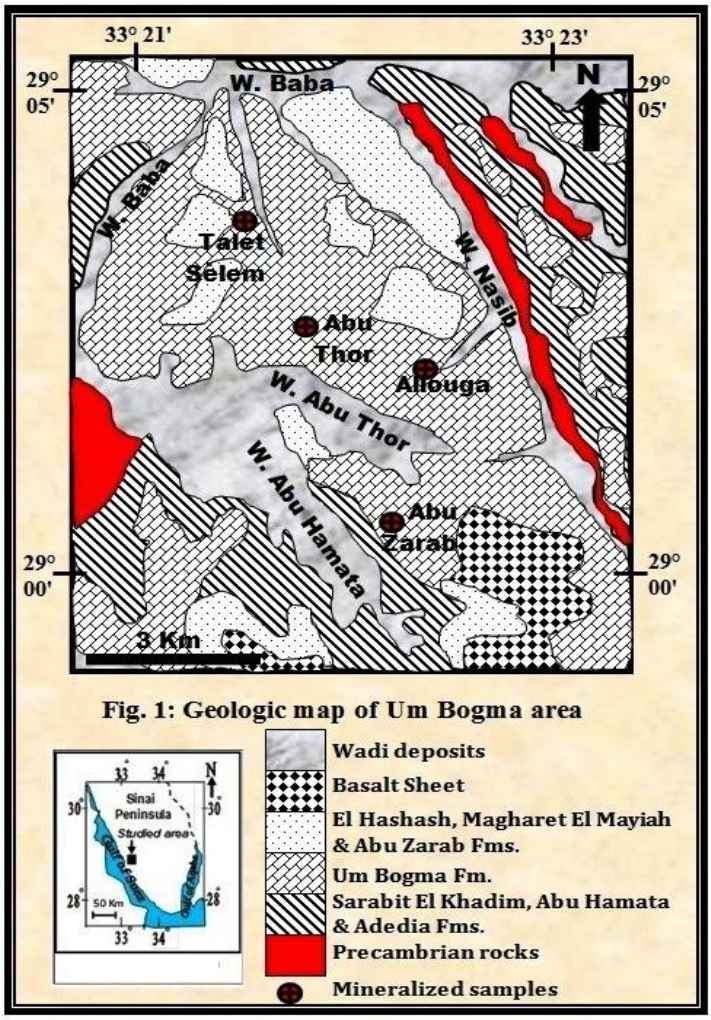

Fig. 1: Geologic map of Um Bogma area

SW Sinai considered an important target for some economic ores as copper, coal, kaolin, manganese, glass sand and recently REEs, uranium, thorium and gold, the lithology, structure and topography played an important role in localization of uranium and associated element **(Alshami 2017)**.

Um Bogma area reveals moderate to low topography and covered in part by Precambrian rocks nonconformably by Paleozoic succession.The Paleozoic sediments were classified into Lower Sandstone, Middle Carbonate, and Upper Sandstone, **(Barron, 1907).** The Middle Carbonate Series was found to contain economic Mn-ores. The Carboniferous age was assigned by **(Issawi and Jux, 1982). Weissbroad (1969)** applied the term Um Bogma Formation to the Middle Carbonate Series, which was customized by (**Soliman and Fetouh, 1969; El Shazly, et al, 1974; and Kora 1984). However, Omara and Conil (1965)** classified the Um Bogma Formation into lower dolomitic member, middle dolomitic limestone member and upper dolomitic member. Since, **El Sokkary (1963)** reported some radioactive anomalies discovered in the limestone unit of Um Bogma Formation , more anomalies were discovered at several other localities Allouga, El Sahu, Abu Thor where some yellow and green secondary uranium mineralization were identified **(El Aassy, et al.1986),** and more geologic investigations, were carried out. The detailed stratigraphy of Um Bogma mineralization was identified **(El Aassy, et al. 1986),** and more geologic investigations, were carried out.

Geologic setting

The Paleozoic succession at Um Bogma area comprises seven formations, from base to top as the follow: Sarabit El Khadim, Abu Hamata, Adedia, Um Bogma, El Hashash, Magharet El Mayiah and Abu Zarab Formations (Fig. 1).Um Bogma Formation is the most important formation in the Paleozoic succession from the radioactivity and mineralization points of view.

Um Bogma Formation

In the study area, Um Bogma Formation unconformably overlies Adedia Formation and underlies Abu Thora Formation. Several authors subdivided Um Bogma Formation into either four members ***(Wiessbrod, 1969,***

and Mart and Sass, 1972) or three members ***(Omara and Conil, 1965, and Kora, 1984)***. In this article the authors agree with classification of ***Kora 1984*** which is from base to top as follows:-

The lower member is rest unconformably on Adedia Formation with distinguishable contact due to different lithology. It is enriched by manganese and iron ores. This member exhibits three different lithologic facies include a) Mn-Fe ore, ferruginous siltstone and silty shale facies with black, black brown and reddish brown colors (Fig.2A); b) sandy dolostone facies, it is reveals thick bedded, pink color and sometimes shows horizontally laminated; c) black carbonaceous shale and siltstone facies (Fig. 2B)with patches of copper mineralization (Fig. 2C). Mn- Fe Ore is widely distributed at Allouga and Abu Thor areas and show lenses of high radioactivity in some parts.

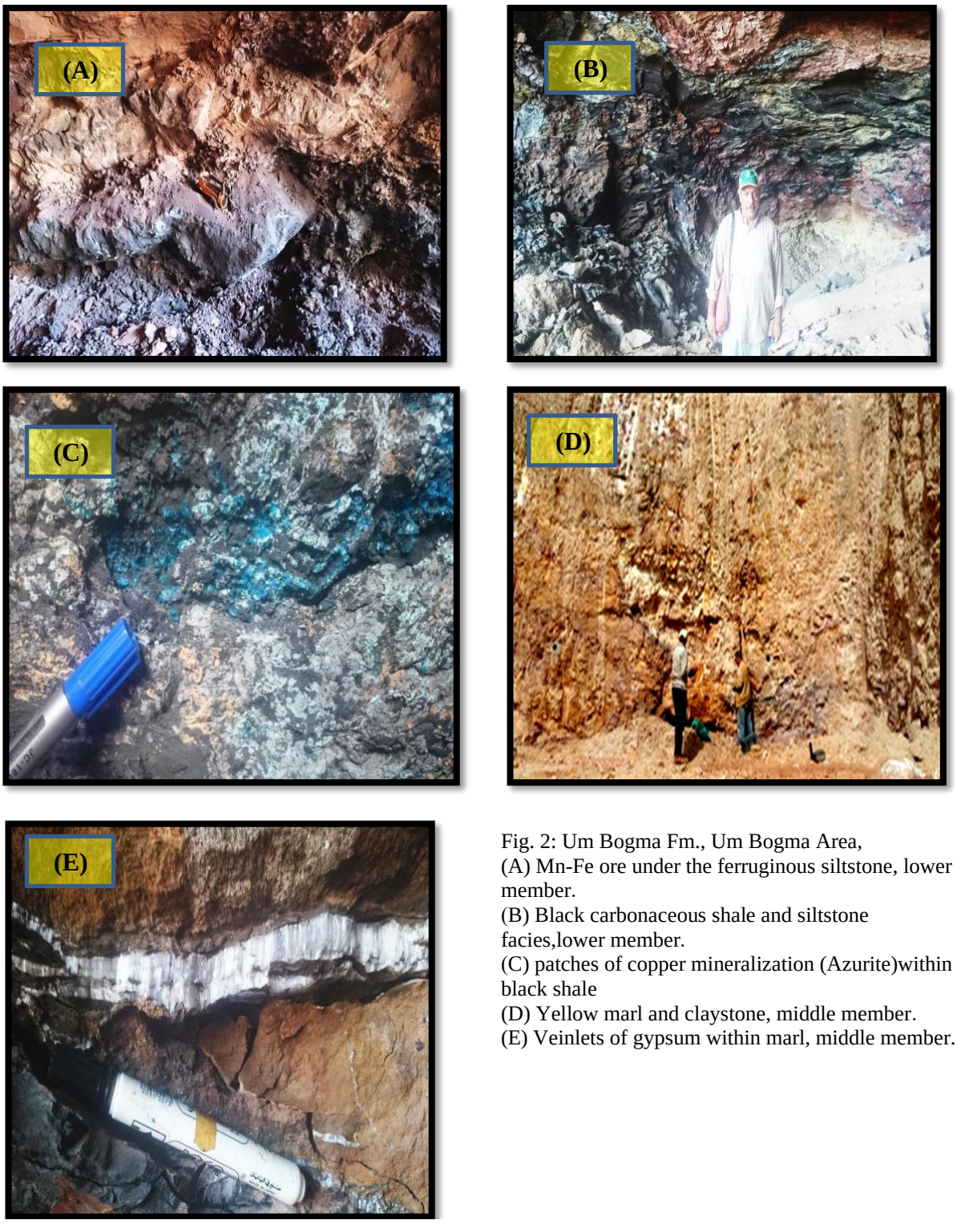

Fig. 2: Um Bogma Fm., Um Bogma Area,
(A) Mn-Fe ore under the ferruginous siltstone, lower member.
(B) Black carbonaceous shale and siltstone facies,lower member.
(C) patches of copper mineralization (Azurite)within black shale
(D) Yellow marl and claystone, middle member.
(E) Veinlets of gypsum within marl, middle member.

The middle member is composed of yellow marl and claystone(Fig. 2D) with fossils content such as Corals, Crinoids, Brachiopods and Mollusca. The middle member is characterized by found of distribution of evaporate minerals as gypsum (Fig. 2E), anhydrite and halite minerals in fibrous and platy habits in the form of parallel veinlets and/or intersection with bedding planes. Also, white and black gibbsite horizon was observed at the boundary between middle member and lower member of Um Bogma Formation with high radioactive anomalies.
The upper member is composed of yellow, pink, and grayish crystalline dolostone, claystone and shale. It is overlies conformably the middle member and reveals cliff and step outcrop. The upper member of Um Bogma Formation can be lithologically subdivided into three lithofacies include, a) medium crystalline dolomite facies, b) sandy dolostone association facies, c) quartz-wake association facies.
The marl unit of the middle member of Um Bogma Formation has wide exposure and highest thickness and radioactivity. So, four localities were chosen for detailed radiometrical, mineralogical and geochemical and studies: Talet Seliem, Abu Thor, Allouga and Abu Zarab.
Four lithostratigraphic sections were constructed for the four localities (Fig. 3). Adedia Formation is exposed at Tatel Seliem, Allouga and Abu Thor locality ranging in thickness from 0.5 to 2 m and composed mainly of ferruginous sandstone. Lower Um Bogma Formation is ranging from 4 to 11 m and decreasing towered the north.It composed mainly of dolostone and Mn-Fe ore at all the chosen localities except Talet Seliem in which the Mn-Fe ore replaced by ferruginous siltstone. Middle Um Bogma Formation reaches the maximum thickness at Abu Thor locality (about 12 m), marl and claystone are the main components. On the other hand, upper Um Bogma Formation reaches 6m in thickness at Talet Seliem locality and composed of claystone and dolostone at Talet Seliem and Abu Thor localities and claystone and shale at Allouga locality, while Abu Zarab locality composed mainly of dolostone.

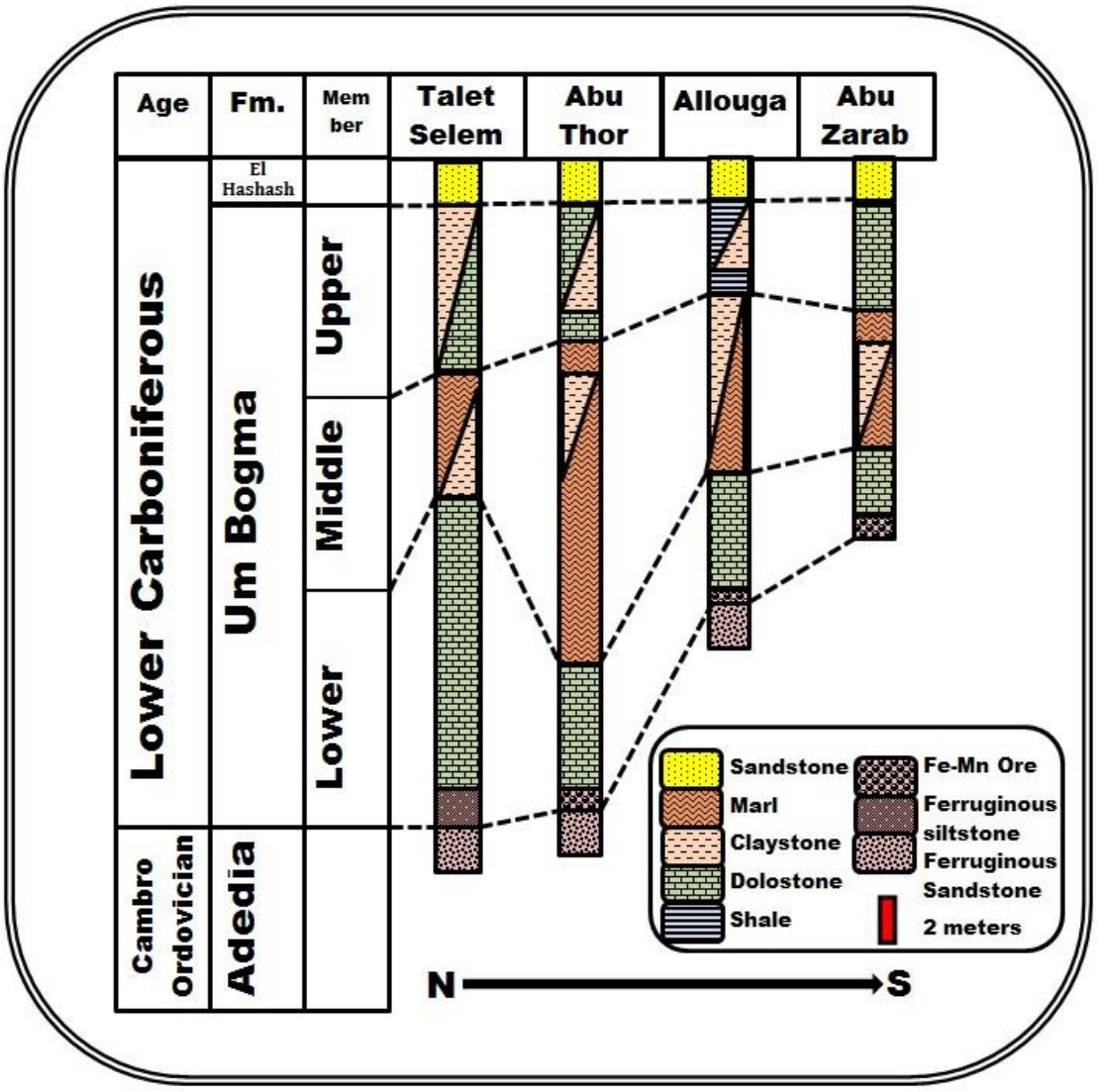

Fig. 3: Stratigraphic correlation of Um Bogma Formation of the study area.

II. Methodology

The field radiometric measurements of eU (ppm), eTh (ppm) and K% were obtained using a portable differential gamma ray spectrometer model Rs-230 BGO Super-Spec, serial No. 4333, manufactured by Radiation Detection Systems AB, Backehagen 35, SE-79191 FALUN, Sweden and the reading were given directly each 30 second.Radioelement concentrations were determined radiometrically by gamma-ray spectrometry using Na-I detector and chemically in ACME analytical Laboratories of Vandcouver, Canada and Nuclear Materials Authority Labs by ICP- emission spectrometry (ICP-ES) and ICP-mass spectrometry (ICP-MS).Uranium content of the collected samples was measured chemically in the laboratories of the Nuclear Materials Authority (NMA), Cairo, Egypt.

All the samples were chemically analyzed, trace elements were measured using X-ray fluorescence (XRF) and atomic absorption and the rare earth elements (REE) were estimated by ACME Laboratories Canada.

For measuring gold, fire assay analyses were carried out at the Egyptian Mineral Resources Authority (EMRA), Central Laboratory Sector. Weigh 50 gm of sample. Addition of flux (litharge- Borax –Sodium carbonate –Flour –Silica – silver).Mix sample with flux in ceramic crucible.Melting of (sample + flux) at 1000^0 C for 1.5 hours. Cupellation of (lead + gold +silver) alloy at 900^0 C for 1 hour.Parting of resulting (gold –silver) alloy in Nitric acid and aqua regia heating to get gold solution. Analysis of gold solution by GBC Avanta atomic absorption instrument to get gold concentration with ppm.

The anomalous samples, whether soft or hard, were collected (weighting from 3 to 5kg for each sample). In order to determine their mineralogical constituents; the samples were crushed and screened.The fractions having grain size range between 0.074mm and 0.5mm were used. These size fractions were subjected to systematic mineral separation techniques using bromoform (Sp.G. = 2.85) as a heavy liquid and magnetic fractionation using Frantz Isodynamic Magnetic Separator at side slope of 5^o, forward slope of 20^o and 0.5 A ***(Flinter, 1959)***.

The obtained heavy mineral fractions were studied under the Binocular microscope and Environmental Scanning Electron Microscope (XL30-ESEM, Philips) attached with EDAX microanalysis unit developments in high-pressure (low-vacuum). These analyses were carried out in the laboratories of the Nuclear Materials Authority (NMA), Cairo, Egypt. While, the polished sections were studied under the Scanning electron microscopy (Quanta FEG 200, FEI France, Thermo Fisher Scientific, Mérignac, France) while element analysis was obtained using an Oxford Inca 350 EDX microanalyzer (connected to SEM, Oxford Instruments France, Saclay, France).

Radioactivity

The radiometric measurements of the anomalous samples for the studied localities (Table 1) show that the radioelement contents in marl of Talet Seliem area range between 486 and 810 ppm for U, 0.2 and 0.5 ppm for Th, 452 and 714 ppm for RaeU, in addition to 0.93 and 2.01 % for K. Abu Thour locality contains lower U, Ra and K and higher Th contents than Talet Seliem, where uranium concentrations range between 133 and 151 ppm, Th between 0.44 and 12 ppm, RaeU between 220 and 232 ppm while K between 0.31 and 1%.

Abu Zarab marl is considered the lowest in uranium and RaeU contents in comparison with the studied localities, where uranium varies between 56 and 143 ppm, Th between 2 and 25 ppm, RaeU between 51 and 87 ppm but K between 0.1 and 1.4 %. On the other hand, Allouga locality marl has the highest U, Th, RaeU and K concentrations in comparison with all the studied localities resulting from its high radioactive minerals contents as indicated in the mineralogical studies.

The eU/eTh ratio is an important radiometric parameter to identify the sites of U-mineralization. It is used also to detect the oxidation state in which U transported **(Naumov, 1959)**. The productive uraniferous rocks have U/Th ratio > 1 **(Darnely and Ford, 1989)**.

The examined marl of the studied localities exhibit eU/eTh ratio ranging between 1490 and 2430 with an average of 1973 ppm for Talet Seliem, between 11.92 and 343.18 with 145.36 ppm for Abu Thour, between 5.09 and 31 with an average 15.58 ppm for Abu Zarab and between 8.09 and 4339.39 with an average 1140.46 ppm for Allouga locality (Table 1). This means that, the investigated marl is considered as productive uraniferous rocks in all the studied localities, especially Talet Seliem and Allouga which are considered as sites uranium deposition.

From table 1, it can be concluded the lesser values of chemically measured uranium with respect to radiometrically measured indicates uranium migration from the marl to the other rock types in the same formation or other formations (migration out). One sample in Talet Seliem and other one in Allouga show high values of chemically measured uranium with respect to radiometrically measured indicate uranium migration from theother rock types in the same formation or other formations to the marl (migration in).

In contrast to the previous results eU/RaeU suggest uranium deposition in most of the studied localities indicating severe changes in physico-chemical conditions of the studied rocks and disequilibrium.

Table 1: Radiometric and chemical measurements of the anomalous samples, Um Bogma area.

Sample No.	eU ppm	eTh ppm	RaeU ppm	K%	Uc	Uc/eU	eU/eTh	eU/RaeU
TS a	745	0.5	714	0.93			1490.00	**1.04**
TS b	810	0.4	591	2.01	940.5	1.2	2025.00	**1.37**
TS c	486	0.2	452	0.96	420	0.86	2430.00	**1.08**
Min.	486	0.2	452	0.93	420	0.86	1490.00	**1.04**
Max.	810	0.5	714	2.01	940.5	1.2	2430.00	**1.37**
Average	667.4	0.36	584.6	1.368	680.3	1.03	1973.00	**1.18**
AT a	151	0.44	232	0.31	180	1.19	343.18	**0.65**
AT b	143	12	220	1			11.92	**0.65**
AT c	133	8	220	0.66	273.7	2.1	16.63	**0.60**
Min.	133	0.44	220	0.31	180	1.19	11.92	**0.60**
Max.	151	12	232	1	273.7	2.1	343.18	**0.65**
Average	142.2	6.576	224.8	0.656	226.9	1.65	145.36	**0.63**
Ag a	1432	0.33	1157	1.56			4339.39	**1.24**
Ag b	1027	127	1004	1.89	1429.8		8.09	**1.02**
Ag d	1276	19	981	0.12	1150	0.90	67.16	**1.30**
Ag e	1035	38	797	1.06	1031	1.0	27.24	**1.30**
Ag f	637	2	854	3.09			318.50	**0.75**
Ag g	923	53	885	1.7			17.42	**1.04**
Min.	637	2	797	0.12	1031	0.9	8.09	**0.75**
Max.	1276	53	981	3.09	1429.3	1.0	4339.39	**1.30**
Average	964	27.83	882.5	1.57	1203.6	1.0	1140.66	**1.09**
Az a	143	25	51	0.1	125	0.87	5.72	**2.80**
Az b	56	11	76	1.4	91.2	1.63	5.09	**0.74**
Az c	62	2	87	1.19			31.00	**0.71**
Min.	56	2	51	0.1	91.2	0.87	5.09	**0.71**
Max.	143	25	87	1.4	125	1.63	31.00	**2.80**
Average	92	13	70.4	0.838	108.1	1.25	15.58	**1.55**

Ts (Talet Seliem),**At** (Abu Thour), **Ag** (Allouga) and **Az** (Abu Zarab)

III. Mineralogy

Gold

It is present in the four localities with anomalous contents. Polished sections were done for the high gold content samples to study the gold and the associated base metals, elements and minerals by the scanning electron microscope. The ESEM patterns and EDAX data carried out on the chosen spots within the polished sections reveals that native gold present in association of Fe Mn (Fig.3).

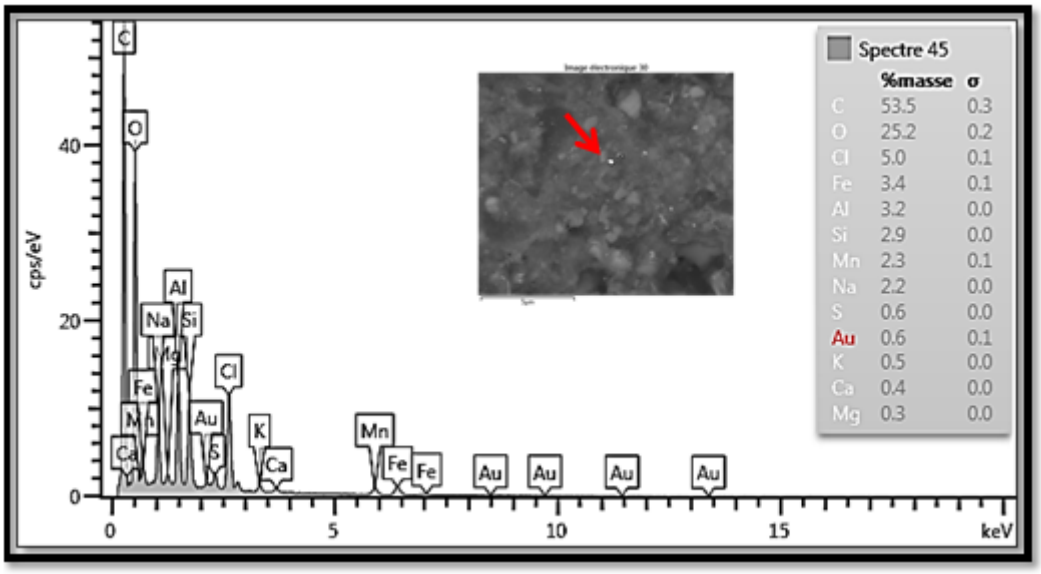

Fig.3: BSE and EDAX of gold.

- **Talet Seliem locality**

The minerals that are identified in Talet Seliem generally represented by autonite, cerianite, pyrite, corandite, iron oxides and clays-bearing REEs and bastanesite.

Autonite [Ca (UO2)2(PO4)2, 8-12H2O]

This mineral is to some extent highly speeded in the oxidation zones of most uranium deposits **(Cesbron et al., 1993).** Autonite crystals are generally of dull luster and present as soft aggregates and encrustations of bright yellow colors (Fig. 4). EDAX analyses confirm the composition of autonite where it is mainly composed of U, P with appreciable amounts of Fe and Cu.

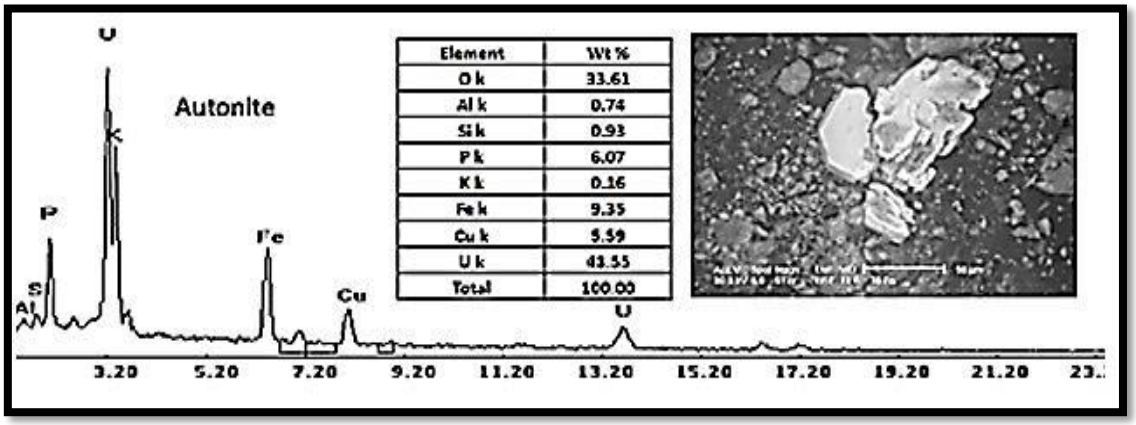

Fig.4: BSE and EDAX of autonite.

Cerlanite (Ce-oxide mineral)

Cerlanite is a sensitive indicator of conditions of mineral formation, because Ce is the only compatible REE, which in natural conditions can occur not only in trivalent but also in tetravalent form. Cerlanite is formed only in strongly oxidizing conditions, mainly in alkaline solutions (fluids) **(Akagi and Masuda, 1998)**. Cerlanite is found as the main REE where Ce reaches up to 70.29 wt.% with appreciable amount of Si, Fe, Zn, Mn, Al, Mn, Ca and K (Fig.5).

Pyrite (Fe S2)

Pyrite is the most abundant sulfide minerals in the Earth's surficial rocks. Pyrite forms large bodies in moderate- to high temperature hydrothermal deposits and in contact metamorphic ore deposits. Pyrite occurs as coarse-grained euhedral to subhedral crystals in the studied locality with slightly corroded outlines and includes grains of finer sulphides. EDAX analyses confirm the composition of pyrite (Fig. 5).

Corandite $Pb(Mn^{4+},Mn^{2+})_8O_6$

Corandite is an admixture between Mn, and Pb oxides with impurities of Fe, Al, S and Zn **(Betekhtian, 1973)**. It has Dark grey, black colour and sub-metallic, dull luster with massive, betroidal crusts and fibrous structure. Corandite is a primary mineral in hydrothermal veins, secondary origin in oxidized zones above Mn deposits and bedded sedimentary rocks. EDAX analyses clarify its composition where it contains Pb, Mn, Fe, Cl and Mg as essential components with subordinate amounts of Al and Ca (Fig.5).

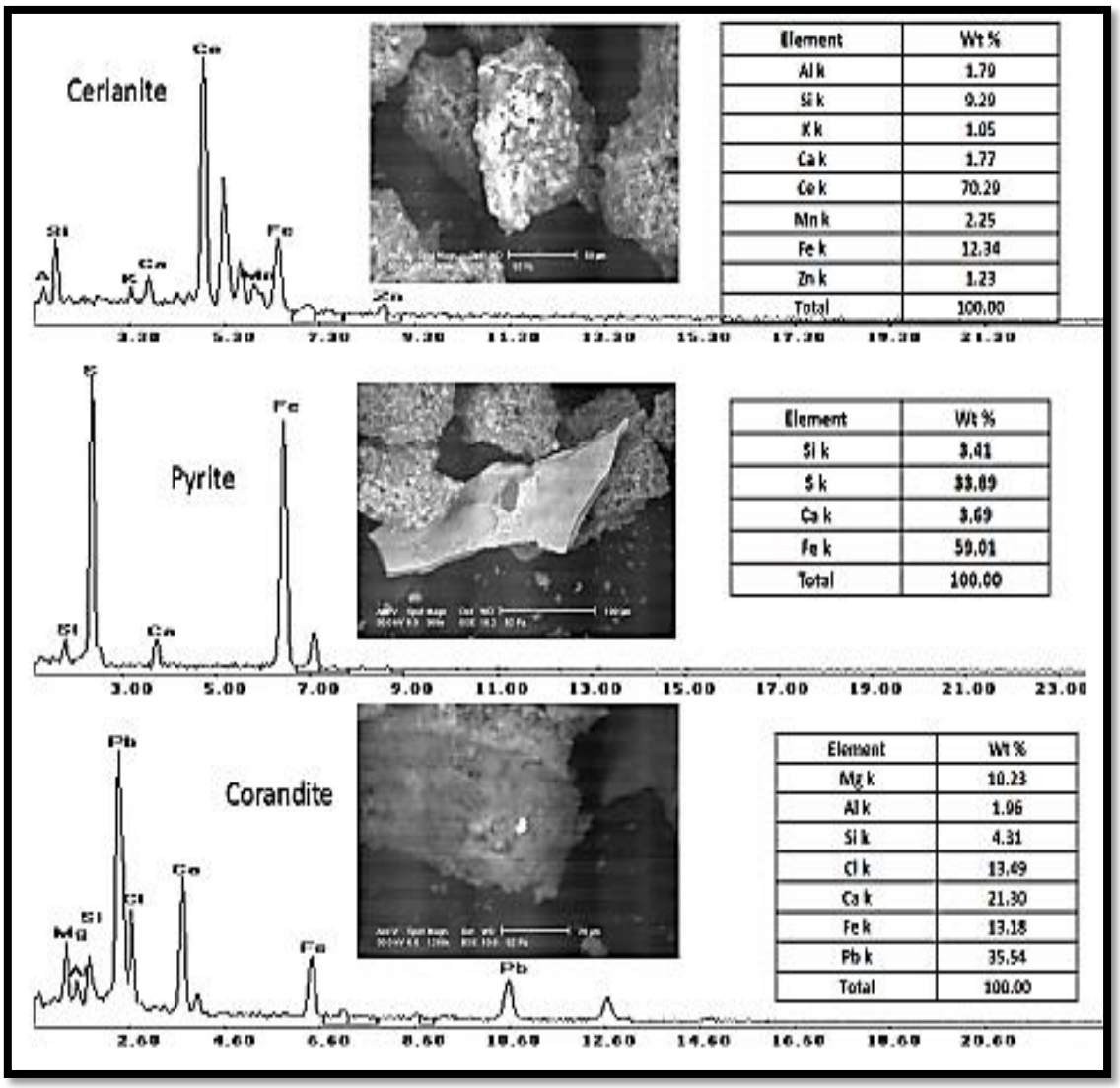

Fig. 5: BSE and EDAX of cerianite, pyrite and carondite.

Iron oxides and clays-bearing REEs

It is found that iron oxides and clays scavenge high contents of REEs as shown from EDAX analyses (Fig.6).

Bastnaesite

Bastnaesite is the fluorocarbonate of lanthanum and cerium. It is the most economically signiicant mineral of more than 200 minerals known to contain essential or significant REE, where it is a potential source of the LREE and account for about 95% of the REE currently utilized in the world. It occurs as elliptical aggregates and encrustations with waxy-yellow to reddish-brown color and commonly associated with zinc ores. EDAX analyses emphasize the composition of bastanesite(Fig.6).

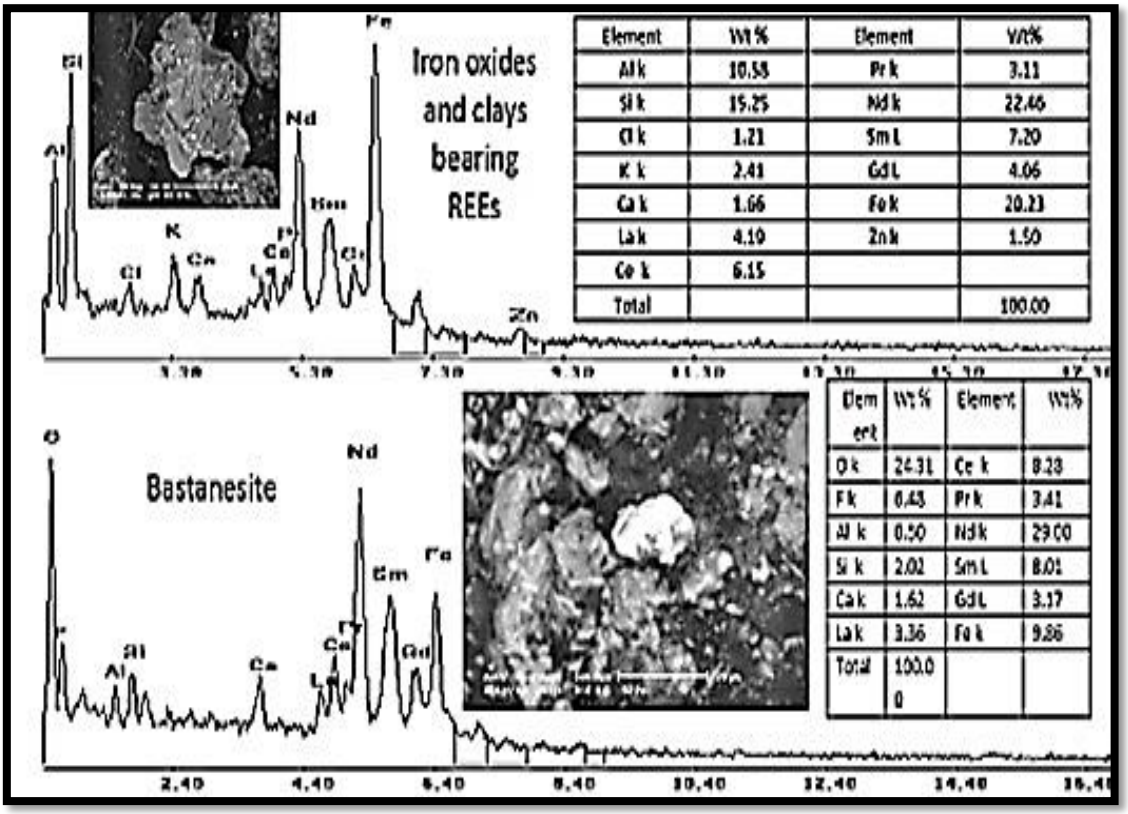

Fig.6: BSE and EDAX of REEs and bastansite.

- **Abu Thor locality**

The minerals that are identified in Abu Thor generally represented by REEs mainly Nd adsorbed on clay and gypsum, aurorite and monazite**.**

REEs adsorbed on clay and gypsum:

Clays and gypsum have high ability to adsorb REEs especially Nd as indicated from the correlation coefficient between K, Na and Ca with Nd which are 0.66, 0.98, 0.98, respectively. EDAX analyses indicate this correlation and confirm Nd enrichment in Um Bogma Formation (Fig. 7).

Aurorite [(Mn,Ag,Ca)3O7.3H2O]:

It occurs as splotchy, anhedral crystals forming inclusions in calcite and other minerals. It has black to blackish grey color. EDAX analyses show that this mineral is mainly composed of Ag, Ca with Si, Al, Mg, Al, Na, S and Cl (Fig. 7). This mineral was also identified by **Monem et al., (1997)** and **Dawood (2005).**

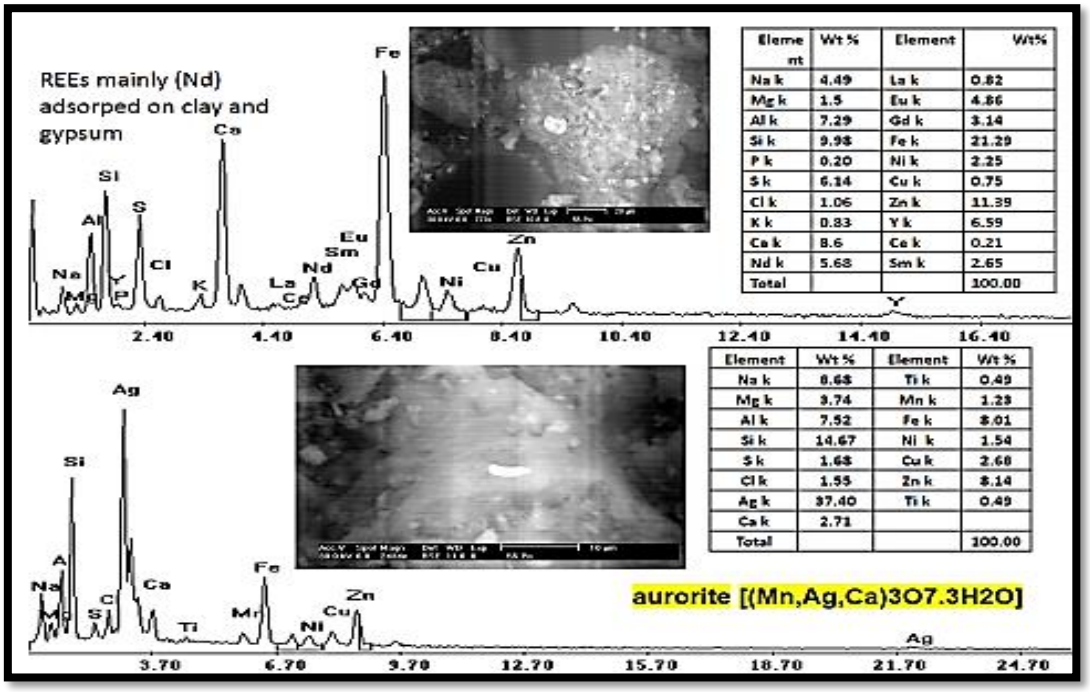

Element	Wt %	Element	Wt%
Na k	4.49	La k	0.82
Mg k	1.5	Eu k	4.86
Al k	7.29	Gd k	3.14
Si k	9.98	Fe k	21.29
P k	0.20	Ni k	2.25
S k	6.14	Cu k	0.75
Cl k	1.06	Zn k	11.39
K k	0.83	Y k	6.59
Ca k	8.6	Ce k	0.21
Nd k	5.68	Sm k	2.65
Total			100.00

Element	Wt %	Element	Wt %
Na k	8.68	Ti k	0.49
Mg k	3.74	Mn k	1.23
Al k	7.52	Fe k	8.01
Si k	14.67	Ni k	1.54
S k	1.68	Cu k	2.68
Cl k	1.55	Zn k	8.14
Ag k	37.40	Ti k	0.49
Ca k	2.71		
Total			100.00

Fig.7: BSE and EDAX of REEs, gypsum and aurorite.

Monazite (Ce, La, Th) PO4

Monazite is phosphate mineral which attains special importance of rare elements such as thorium and REE, especially lanthanum and cerium while uranium is present in small amounts **(Bee, 1996).** It is the most common REE-bearing mineral, which has preferential selectivity towards the LREE and is also known as ultra-stable mineral during weathering. Monazite is transparent with vitreous luster, pale to honey yellow grains. From EDAX analyses, it is clear that this mineral is mainly composed of La as the sole LREE, in addition to the presence of Ca, Na, Mg, Si and S (Fig. 8).

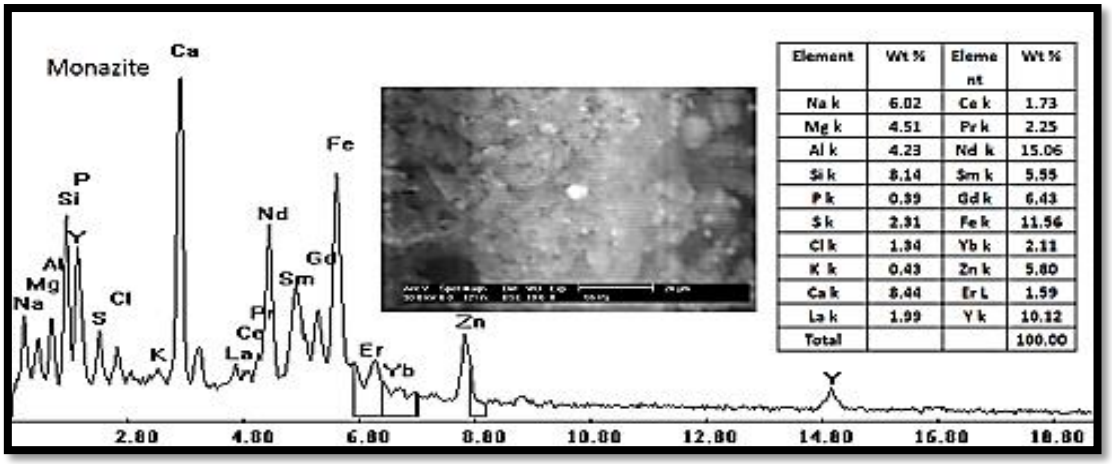

Element	Wt %	Element	Wt %
Na k	6.02	Ce k	1.73
Mg k	4.51	Pr k	2.25
Al k	4.23	Nd k	15.06
Si k	8.14	Sm k	5.55
P k	0.39	Gd k	6.43
S k	2.31	Fe k	11.56
Cl k	1.34	Yb k	2.11
K k	0.43	Zn k	5.80
Ca k	8.44	Er L	1.59
La k	1.99	Y k	10.12
Total			100.00

Fig.8: BSE and EDAX of monazite.

- **Allouga locality**

The main minerals that are registered in Allouga are mainly represented by brannerite, uraninite, carnotite and torbernite**.**

Brannerite

Brannerite (U,Ca,Ce)(Ti,Fe)2O6 represents one of the reduced forms U mineral varities and its U content may be partially oxidized. Uranium is partially replaced by Ca and REE. It occurs as vermiform aggregates suggesting their biogenic origin where these aggregates are of submicroscopic vision. EDAX analyses indicate that this mineral is mainly composed of U, Ca, Fe and Ti with appreciable amount of Si, Al, Kand Na from clays in which it immersed (Fig. 9).

Uraninite

Uraninite is the major ore mineral of uranium. Uraninite occurs as black, gray, or brown metamict crystals that are moderately hard and generally opaque and as black inclusions. EDAX analyses clarify that this mineral contains uranium and oxygen as essential components, in addition to Si, Al, K, Fe, S and Na. the presence of sulpher and iron indicate the role of pyrite as reducing agent that help in uraninite formation (Fig. 9). This mineral was previously identified by **Beshr (2012).**

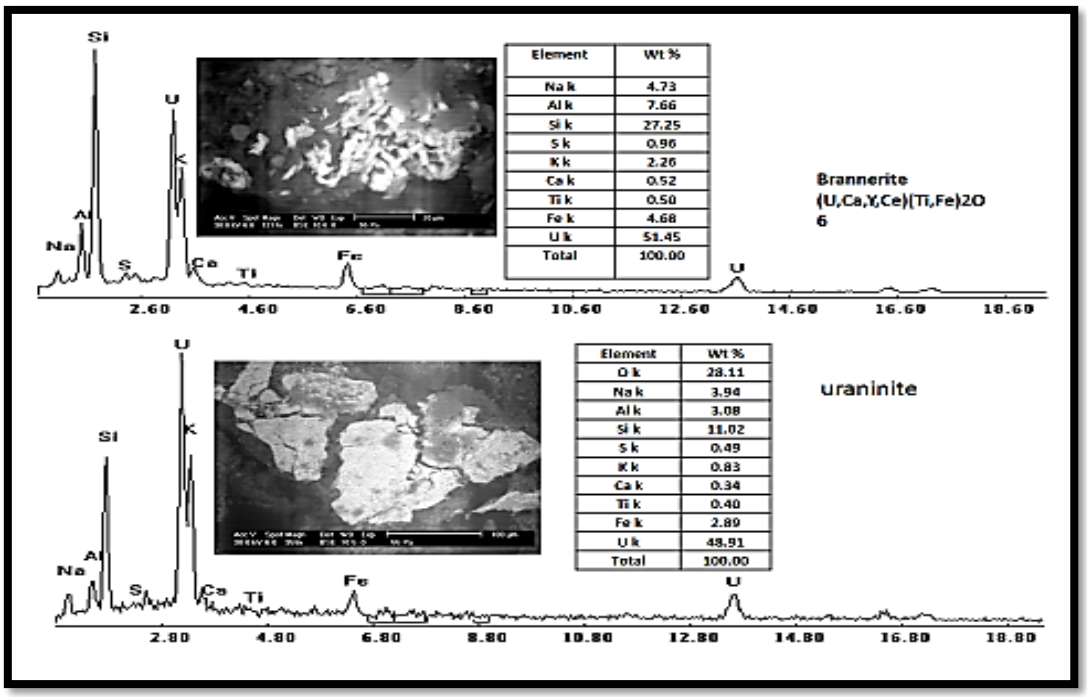

Fig.9: BSE and EDAX of brannerite and uraninite.

Torbernite

Torbernite [Cu U_2 $P0_4$) is widely spread in the Allouga area. Torbernite occurs as fracture filling. It is bright blue to green, transparent to translucent, tabular mineral and as leaf'-shaped crystals (Fig.10). Torbernite is identified by binuclear microscope and X-ray diffraction analyses (Fig. 10&11).

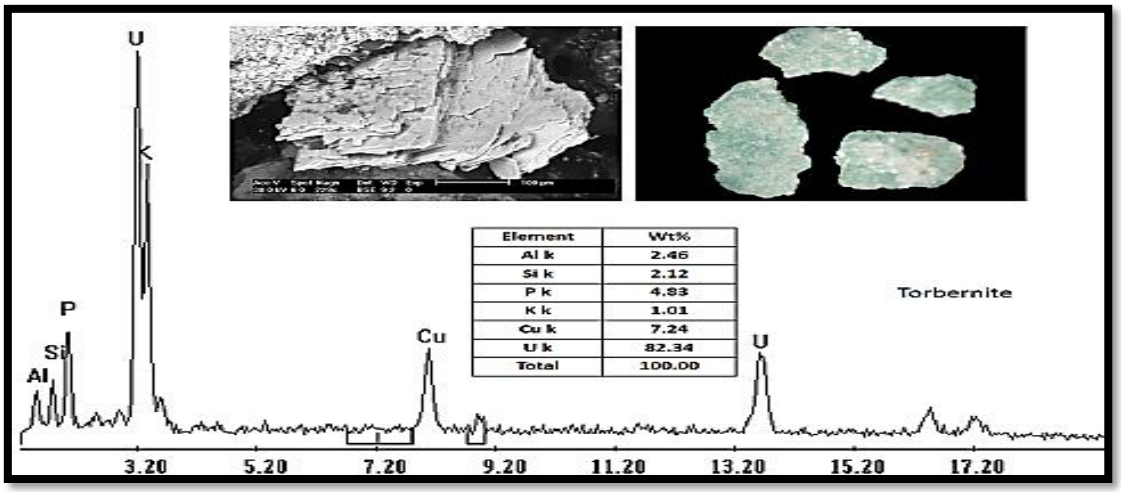

Fig.10: Picked grains, BSE and EDAX of torbernite.

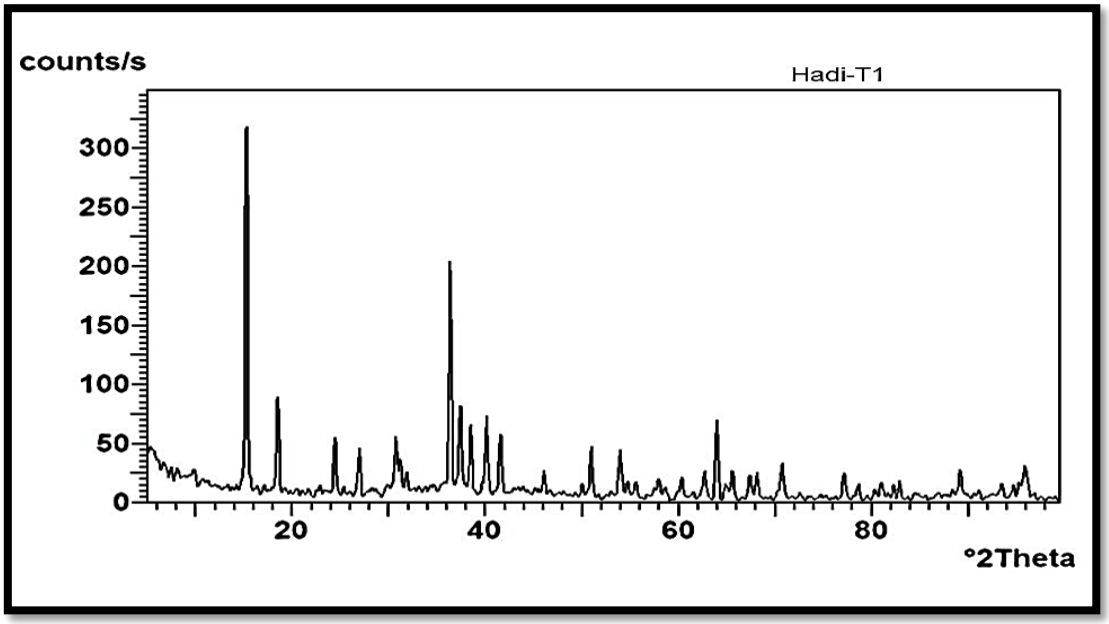

Fig. 11: X-ray diffraction pattern of torbernite.

Carnotite

Carnotite ($K_2(UO_2)$ (VO4) nH_2O) , a potassium uranium vanadate, is the most important of the secondary uranium ore minerals. It is a lemon-yellow mineral with an earthy luster, a yellow streak (Fig.12). It occurs most commonly in soft; powdery aggregates of finely crystalline material or in thin films. The occurrence of carnotite was also confirmed by X-ray diffraction analyses (Fig. 13).

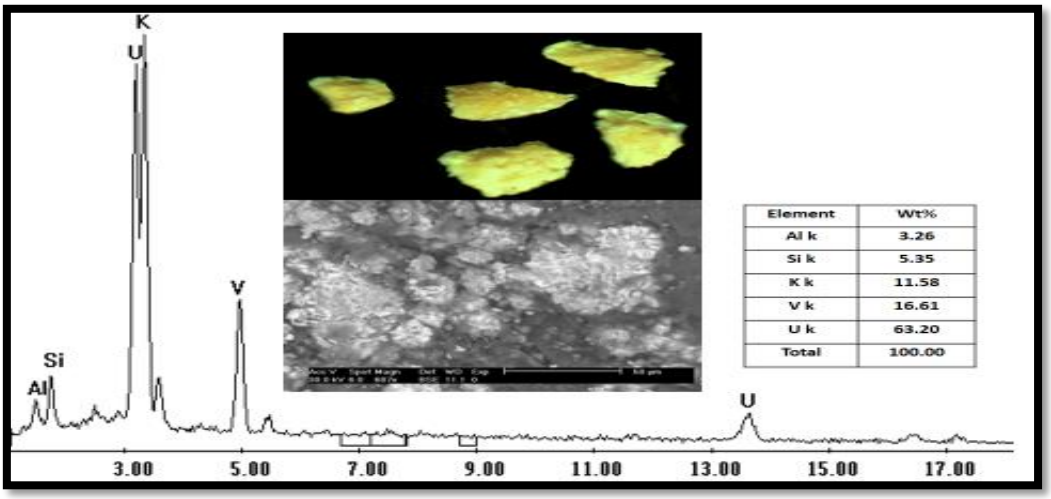

Fig.12: Picked grains, BSE and EDAX of carnotite.

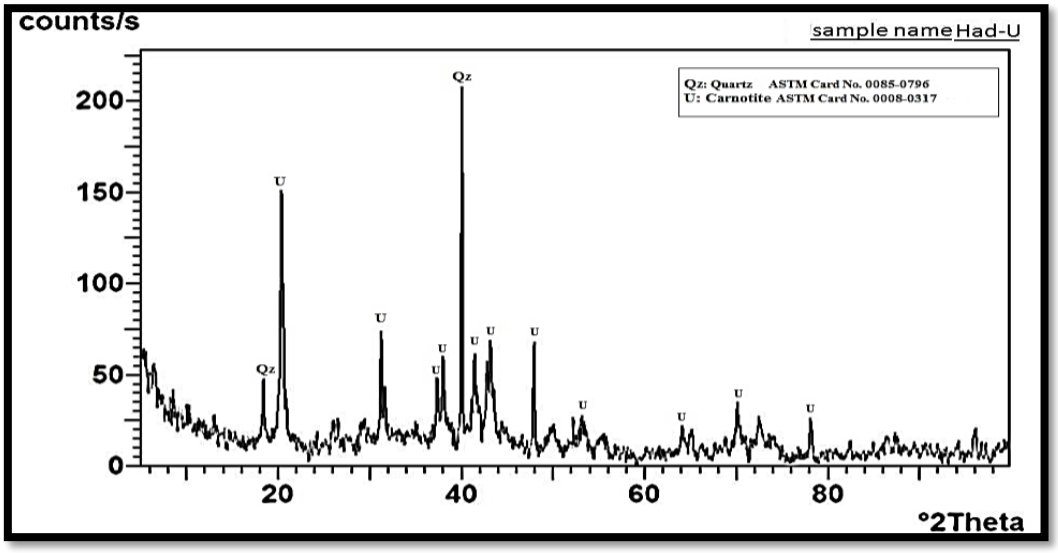

Fig**. 13:** X-ray diffraction pattern of carnotite

• **Abu Zarab locality**

The main minerals that are registered in Allouga are mainly represented by thorite, paratacamite, malachite, galena and jarosite**.**

Thorite (Th, U) SiO_4

Thorite occurs as fine yellowish orange grains. The EDAX analyses shows that it consists essentially of Th and U with Si, Al, Y, Ce, Sn and lesser amounts of Ca and S (Fig. 14).

Paratacamite $Cu_2Cl(OH)_3$

Atacamite is a copper halide mineral. Atacamite is of bright to dark green elongated fibrous aggregates or as massive crusts of sub-parallel crystals and coatings on other minerals. This mineral is mainly composed of Cu (Fig. 14&15).

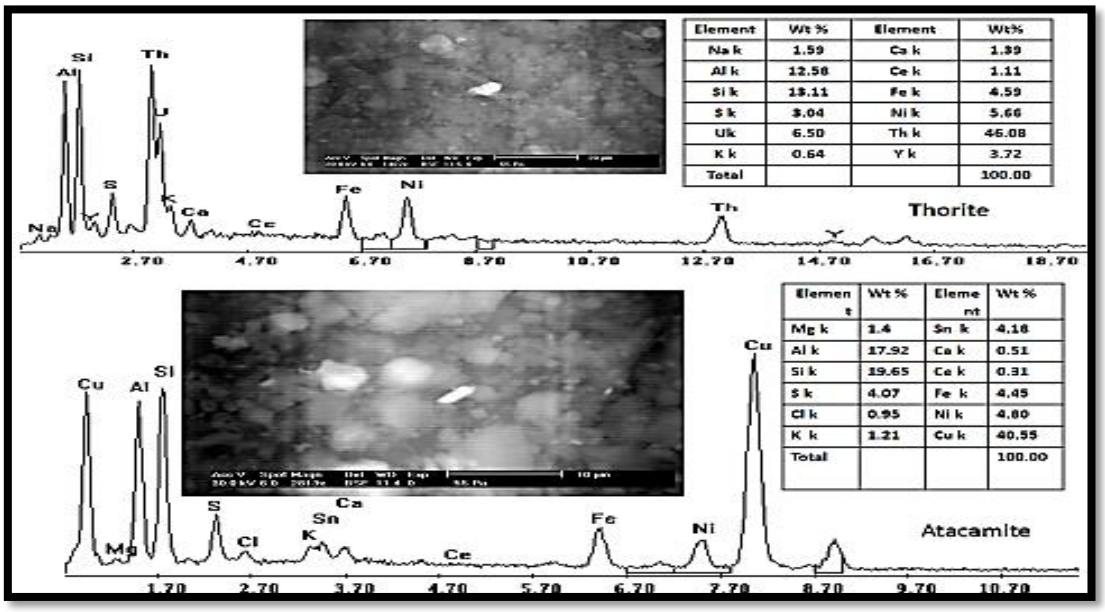

Fig.14: BSE and EDAX of thorite and atacamite.

Malachite $Cu_2CO_3(OH)_2$

Malachite is the predominant ore of copper. It is non-opaque and occurs as prismatic, thick tabular and sometime rounded to sub- rounded, bright green, dark green, green to yellowish green color grains. The presence of paratacamite in association with malachite was confirmed by X-ray diffraction analyses (Fig. 15).

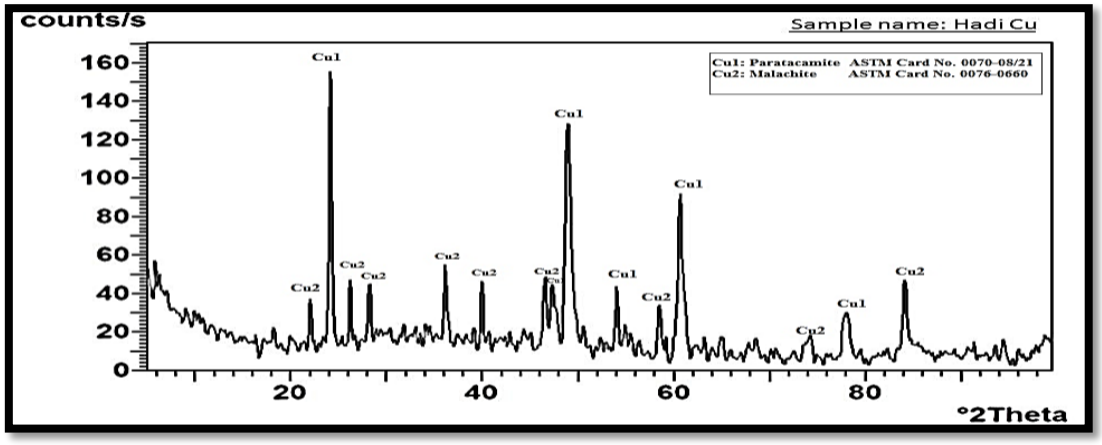

Fig.15: X-ray diffraction pattern of paratacamite and malachite

Galena (PbS)

Galena is a lead sulfide mineral. Lead grey galena grains with sub-metallic luster occur with appreciable amounts. Lead and sulphur are the main components as indicated from EDAX analyses (Fig. 16).

Jarosite [K Fe_3 $(SO_4)_2$ $(OH)_6$

Jarosite occurs as massive to granular form ranging in color from dark yellow to yellowish brown with vitreous to dull luster. It commonly occurs as secondary mineral in acidic and sulphate rich environments. It is enriched in Tl as indicated from EDAX analyses (Fig. 16).

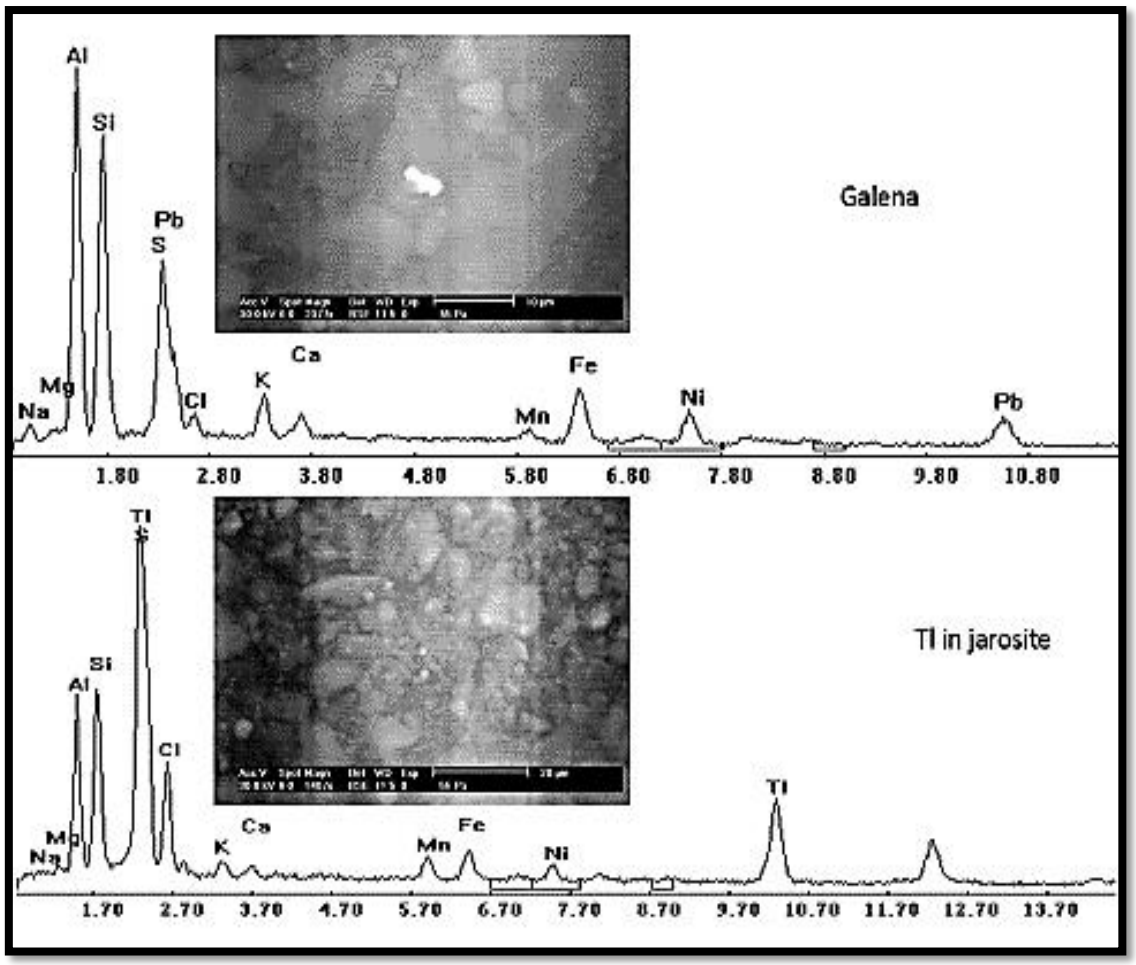

Fig.16: BSE and EDAX of galena and jarosite.

IV. Geochemistry

Chemical analyses of major oxides (%), trace and rear earth elements of the studied samples are cared out in Table 2.

Major oxides

Major element oxide concentrations of Talet Seliem, Abu Zarab, Abu Thour and Allouga marl are listed in Table and are relatively varied. The SiO_2 concentrations range from 24.18 in Talet Seliem locality to 39.50 wt.% in Abu Zarab locality, and the Al_2O_3 concentrations ranges are 9.37-21.65 wt.% in Abu Thour and Abu Zarab localities, respectively, while $Fe_2O_3^t$ ranges are 10.14-23.86 wt.% in Abu Zarab and Talet Seliem localities, respectively.

The CaO and MgO concentrations have ranges of 0.43-10.75 wt.%, 0.96-1.27 wt.%, in Talet Seliem and Abu Thour localities, respectively. Na_2O varies between 0.56 and 1.29 wt.% in Allouga and Talet Seliem where K_2O ranges are 0.80 and 2.61 wt.%, respectively. The TiO_2 varies from 0.30 to 0.83 wt.% in Abu Thou and Abu Zarab localities, respectively P2O5 and MnO contents are very low on contrast to high L.O.I. values in the studied localities.

Trace elements

The Zr and Hf concentration values vary from 103.3-357.1 ppm and 2.64-9.70 ppm in Abu Thour and Allouga localities, respectively (Table 2). The values of Y vary within the ranges of 55.6‑566.5 ppm in Allouga and Talet Seliem localities, respectively. The values of Nb and Ta in the studied localities lie within the ranges of 13.71‑50.82 ppm and1.0‑3.4ppm, in Abu Thour and Allouga localities, respectively (Table 2).

These localities recorded high uranium and low concentrations where uranium value ranges are 91.2 and 1429.8 ppm in Abu Zarab and Allouga localities, respectively but thorium ranges are 7.1-21.8 in in Abu Thour and Allouga localities, respectively. Zn concentrations are very high and reach up to >10000 in Talet Seliem and Abu Thour localities, respectively. Cu, As and Co contents that reach up to 3241.1, 257.4 and 1468.4 ppm in Allouga, for Cu and As and Abu Thour for Co. It is notable that, the toxic elements Cd, Pb and As are high in these localities.

Table 2: Chemical analyses of major oxides (%), trace and rear earth elements\ of the studied samples, Um Bogma area.

Locality	Talet Seliem	Abu Thour	Allouga	Abu Zarab
Rock type	Marl			
SiO_2	24.18	28.18	28.5	39.5
Al_2O_3	16.268	9.372	13.831	21.653
TiO_2	0.647	0.305	0.832	0.380
$Fe_2O_3^t$	23.86	12.27	11.71	10.14
MgO	0.962	1.277	1.177	0.597
CaO	0.434	10.75	0.895	1.987
Na_2O	1.293	1.069	0.566	1.805
K_2O	1.830	0.807	2.614	1.457
MnO	0.075	1.291	0.067	1.291
P_2O_5	0.105	0.119	0.359	0.144
L.O.I.	30.35	34.56	39.45	21.04

Table 2: Cont.

Locality	Talet Seliem	Abu Thour	Allouga	Abu Zarab
Rock type	Marl			
Ba	104	42	163	134
Co	149.0	1468.4	65.0	226.3
Cs	9.8	4.7	9.0	4.3
Ga	26.41	7.99	24.94	12.62
Hf	6.59	2.64	9.70	3.78
Nb	38.2	13.71	50.82	20.49
Rb	60.3	25.7	80.7	48.0
Sn	3.2	1.2	4.5	1.8
Sr	154	206	297	477
U	940.5	273.7	1429.8	91.2
Th	15.3	7.1	21.8	10.1
Ta	2.5	1.0	3.4	1.3
Tl	0.388	0.183	0.499	0.228

V	286	190	731	195
W	0.9	0.5	1.2	0.6
Zr	251.6	103.3	357.1	138.3
Mo	92.93	73.85	70.90	123.36
Cu	340.6	1255.0	3241.1	1308.9
Pb	271.01	158.98	230.80	172.59
Zn	>10000	>10000	189.9	5656.4
Ni	732.8	2232.5	60.3	471.0
Bi	0.21	0.09	0.28	0.10
As	217.8	146.1	257.4	195.8
Cd	124.56	17.34	0.40	19.94
Sb	4.18	4.66	4.47	4.98
Cr	227	106	312	162
Be	58	115	10	44
Sc	13.9	4.9	11.9	16.0
Li	17.2	25.3	12.2	26.5
In	0.08	0.02	0.05	0.11
Re	0.009	0.011	<0.002	0.003
Y	556.6	532.2	55.6	87.7

Table 2: Cont.

Locality	**Talet Seliem**	**Abu Thour**	**Allouga**	**Abu Zarab**
Rock type	Marl			
La	323.6	54.3	88.1	85.4
Ce	1372.29	189.97	171.30	189.72
Pr	451.6	34.5	18.5	24.4
Nd	>2000	241.4	74.8	105.1
Sm	1079.3	90.3	14.1	26.0
Eu	176.3	21.3	2.5	5.0
Gd	684.3	147.6	12.6	29.9
Tb	67.6	22.0	1.6	3.9
Dy	264.1	129.7	10.8	21.6
Ho	29.0	21.8	2.1	3.7
Er	59.7	52.4	5.9	8.7
Tm	7.8	6.6	0.8	1.1
Yb	53.4	40.7	5.7	7.0
Lu	5.7	5.2	0.8	0.9
La/Yb_n	0.4	0.1	1.1	0.9
La/Sm_n	0.0	0.1	0.9	0.5
Gd/Yb_n	7.4	2.1	1.3	2.5
Sr/Eu	0.87	9.67	118.80	95.40
Eu/Sm	0.16	0.24	0.18	0.19
Y/Ho	19.19	24.41	26.48	23.70
La/Y	0.58	0.10	1.58	0.97
REE	4574.69	1057.77	409.6	512.42
LREE	3226.79	610.47	366.80	430.62
MREE	4647.19	520.17	352.7	404.62
HREE	1171.60	426.00	40.30	76.80
LREE/HREE	2.75	1.43	9.10	5.61
Ce/Ce*	0.96	0.95	0.92	0.93
Eu/Eu*	1.0	0.8	0.9	0.8
Zr/Hf	38.18	39.13	36.81	36.59
Nb/Ta	15.28	13.71	14.95	15.76
Ba/Sr	0.68	0.20	0.55	0.28
Ba/Rb	1.72	1.63	2.02	2.79
Rb/Sr	0.39	0.12	0.27	0.10
t1	1.15	0.93	0.91	0.94
t3	1.10	1.10	0.94	1.02
$TE_{1..3}$	1.13	1.01	0.92	0.98
t4	1.11	1.06	0.99	1.05
$TE_{1,4}$	1.13	0.99	0.95	0.99

****t1, t3, t4 and t are calculated according to Irber (1999). -: not determined.**

Gold and silver contents

Gold content in the four localities (Talet Seliem, Abu Zarab, Abu Thour and Allouga) was determined for 4 representative samples (Tab. 3). The determination of gold content using the fire assay technique was carried out on bulk samples before mineral separation. Silver contents were determined using ICP-ES and ICP-MS techniques. Gold and silver contents are high in these localities and vary from 1.6 to 1.78 ppm in Abu Thour and Allouga localities, respectively for gold and from 2.01 to 27.15 ppm for silver. These high values of gold and silver mineralizations are recorded for the first time in the marl of middle Um Bogma Formation in the four localities.

Table 3: Gold and silver concentrations in ppm in the studied samples, Um Bogma area.

Locality	Talet Seliem	Abu Thour	Allouga	Abu Zarab
Fm.	**Middle Um Bogma**			
Rock type	Marl			
Au	1.78	1.7	1.78	1.6
Ag	2.522	2.005	27.154	6.950

REE distribution

The ΣREE in the studied localities widely vary within the range of 409.6–4574.69 ppm and were illustrated in table (2), indicating REEs enrichment, especially in Talet Seliem locality. The most two common shapes reported for UCC normalized REE distribution patterns for the four studied localities are the so-called sea water-like and convex up ward ("hat-shaped") (Fig. 17). Convex up ward REE distribution patterns are characterized by enrichment of middle REE (MREE from Sm to Dy) and light REE (LREE from La to Nd), heavy REE (HREE from Ho to Lu) depletion, and by a Ce negative anomaly **(Bau& Dulsky1996; Abedini et al., 2017)**.

The marl samples show HREE depletion relative to the MREE and LREE. On the other hand, the MREE are slightly enriched relative to the HREE. This means that all samples display the hat (bell)-shaped REE distribution pattern (Fig.17). The hat-shaped REE pattern together with a negative Ce anomaly in the marl samples shows preferential incorporation of MREE during prolonged exposure to seawaters **(Auer et al. 2017; Abedini et al., 2017).**

Their REE pattern of Talet Seliem area is well characterized by the M-type tetrad effects displayed in the third and fourth tetrads (Fig. 17 & table 2). Most researchers revealed that granites and igneous systems mostly display the convex (M-shape) tetrad-effects which are associated with mineral phases, crystallization, and fluid-rock and/or solution-rock interactions **(McLennan, 1994; Irber, 1999; Moneckeet al., 2007; Nardi et al., 2012; Abedini et al., 2018)**. According to these investigators, fluid rockor solution-rock can play a pronounced role in generation of tetrad-effects. Hence, existence of M-shape tetrad-effects in the marl samples in the third and fourth tetrads could be inherited from the surrounding granitic rocks.

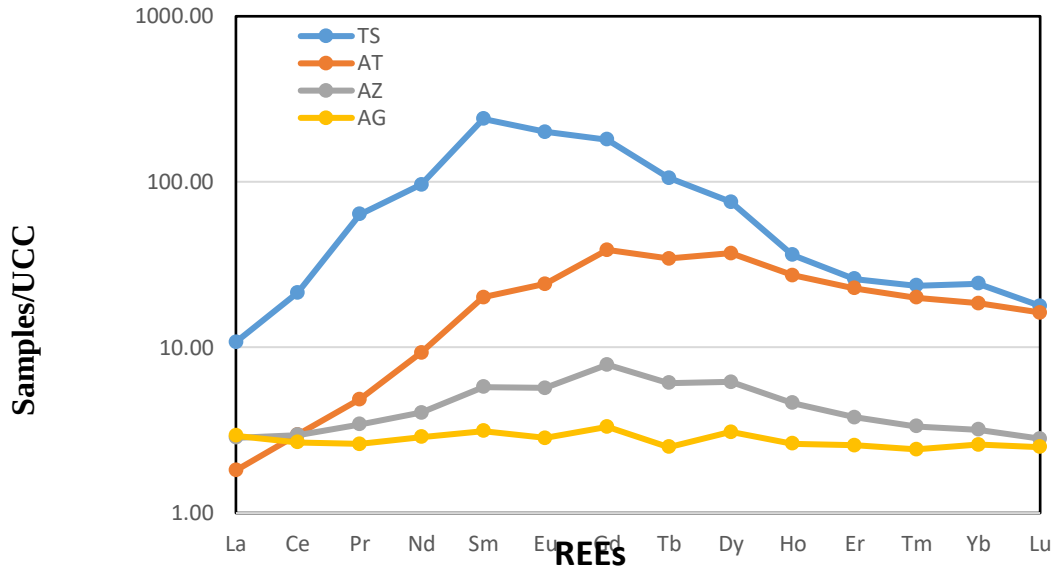

Fig. (17): UCC- normalized REE diagram **(Taylor and. McLennan, 1985)**for the studied localities.

The La/Y and (La/Yb_n) ratios as geochemical parameter have been used to interpret the pH conditions of depositional environment of marl. Values > 1 and< 1 for La/Y ratiois related to alkalic and acidic environment,

respectively (**Crinci and Jurkowic, 1990; Maksimovic and Pantó, 1991).** Values of La/Y and (La/Yb_n) ratios <1 in TaletSeliem, Abu Zarab and Abu Thour marl while La/Y and (La/Yb_n) ratios >1 in Allouga may provide reasons to believe that acidic conditions (due to the dissolved CO_2) were prevailed in the meteoric percolating waters **(Fernandez-Caliani and Cantano, 2010).** These acidic solutions were probably neutralized by rising underground water table level causing the differentiation and enrichment of LREEs and HREEs in the lower parts of Um Bogma Formation.

Therefore, it can be concluded that U and REEs were likely leached from the upper acidic environments (Talet Seliem, Abu Thor and Abu Zarab) and concentrated in the lower alkalic zone under reducing conditions (Allouga), as well as from upper parts of Um Bogma Formation to the lower parts as indicated from geomorphologic studies. Though, REEs in Allouga locality are lesser than other studied localities but **Alshami (2017)** indicated the presence of REEs anomaly in the lower member of Allouga. Consequently, complexion and surface weathering are probable mechanisms to generate the tetrad-effects in the normalized REE patterns of Allouga.

Fractionation of isovalens

The fractionation of elements, which are similar to each other in terms of ionic radius and charge is regarded to be sensitive to changes in melt composition during magma differentiation **(Bau, 1996,1999 and Pan, 1997)**, Y/Ho chondrite ratio is 28 **(Anders and Grevesse, 1989)**. **Bau and Dulski (1995)** suggest complexion with fluorine as major cause for Y/Ho values >28, while the complexion with bicarbonate is assumed to generate Y/Ho values <28. All the studied marl samples have Y/Ho ratios values <28 suggesting the unusual conditions that controlling the Y mobilization with respect to Ho in the studied localities. The lowest value of Y/Ho ratio is found in Talet Seliem area which affected by tetrad phenomena.

Zr and Hf are known to have very similar geochemical behavior, which results in a small range of ratios in geological materials (33–40),**(Jahn et al., 2001)**.In the marl samples, the Zr/Hf ratios (36.59–39.13) are quite normal which could be attributed to the presence of these elements in refractory minerals like zircon.

Sr/Eu chondritic ratio of the marl samples is 139 **(Anders and Grevesses, 1989)**. In the studied samples, the Sr/Eu ranges from 0.87 to 118.80, this may indicate the differential mobility of both Sr and Eu due to pH and oxidation reduction conditions changes.

The studied marl samples show non-chondritic ratio for Nb/Ta (13.71-15.76). The chondritic ratio is 17.6 ±1 for Nb/Ta **(Jahn et al., 2001)**. These non-chondritic ratios are considered as another evidence for physic-chemical changes occurred during the deposition and mineralization of marl.

U/Th ratio of the studied samples range from 9.03 in Abu Zarab to 65.59 ppm in Allouga, which is higher than the average crustal ratio (3.5) of **Roger an Adams (1969)**, suggesting uranium enrichment due to its higher mobility relative thorium during oxidation-reduction condition changes in the environment of deposition.

Geochemistry of major and trace elements in the studied marl:

The results of major, trace and REEs of the studied area are given in Table (2). Geochemically, variations of major, trace and rare earth elements are caused by the loss and gain of elements. To understand the geochemical behavior of major, trace and rare earth elements in the studied localities, it is recommended to normalize this marl to the upper continental crust (UCC) according to **Rudnick and Gao (2003)**.

After that, the reference UCC becomes flat at unity and the relative depletion or enrichment is given by the deviations on both sides of the reference line (Fig.18). Geochemistry of major elements is discussed in terms of gains (positive) and losses (negative) of these elements during marl formation from the mother rocks. Most of clayey marl samples exhibit increase in $Fe_2O_3^t$ and prominent decrease in SiO_2, MgO, Na_2O and K_2O in all the studied localities. Talet Seliem and Abu Zarab show enrichment in Al_2O_3, in contrast to Abu Thour and Allouga.

However, TiO_2 display increase in Talet Seliem and Allouga and decrease in Abu Thour and Abu Zarab. CaO shows enrichment only in Abu Thour locality and depletion in the other localities. Also, P_2O_5 exhibit increase only in Allouga locality and decrease in Talet Seliem, Abu Thour and Abu Zarab. With respect to MnO, it shows enrichment in Abu Thour and Abu Zarab and depletion in Talet Seliem and Allouga.The enhanced Fe_2O_3 content in the in the studied localities may be related to the presence of iron minerals like hematite and goethite formed under suitable Eh-pH conditions during the weathering processes.

Si mass loss indicates kaolinization of feldspars in the studied rocks. The depletion of Na, and K in all the studied localities and Ca in some localities (Fig.18) could be resulted from feldspar alteration and release of these elements into the fluids responsible for alteration. The mass loss of Mg in all the studied localities and Mn in some localities may be resulted from the destruction and alteration of ferromagnesian minerals. The mass gain of Mn in certain localities may be owing to the conversion of Mn2+ to Mn4+ due to change in redox potential condition of the fluids and also to its fixation as insoluble oxides and hydroxides **(Koppi et al. 1996)**.

Formation of titanite is reflected by increased TiO_2 contents in Talet Seliem and Allouga while its depletion in Abu Thour and Abu Zarab localities could be correlated with the destruction of biotite. P_2O_5 depletion in Talet Seliem, Abu Thour and Abu Zarab could be connected with the destruction of apatite while enhanced

values in Allouga are related to the presence of apatite and xenotime as will be illustrated later in the mineralogical studies.

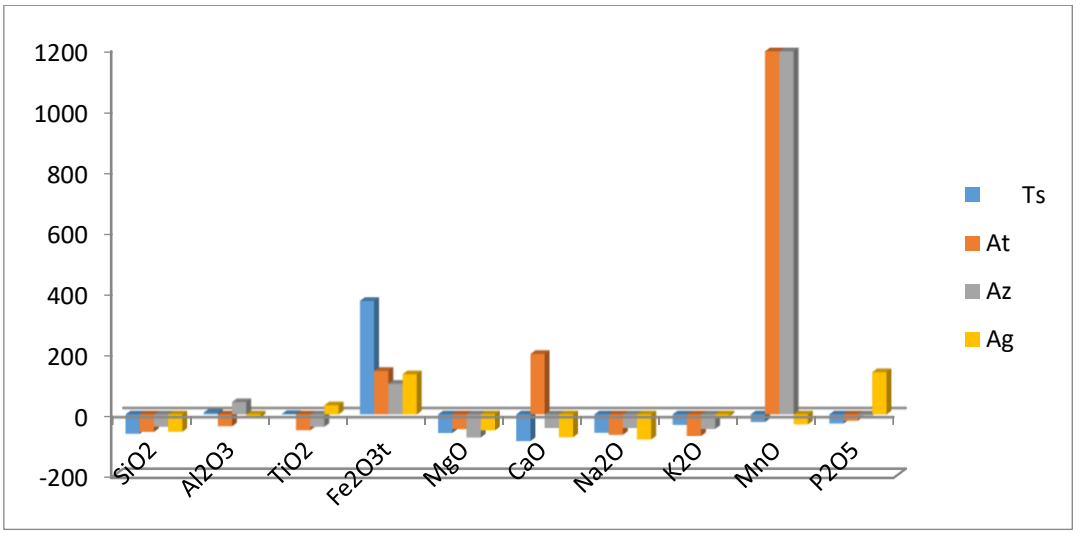

Fig.18: Histogram showing the depletion and enrichment of major oxides of the studied localities.

However, trace elements in the studied samples show enrichment in As, Cd, Sb, Cr, Be, Y, Mo, Ag, Cu, Pb, Zn, Ni, Co, Nb, Ta, U and V whereas they are depleted in Ba, Rb, Sc, Tl and W.Cs, Ga, Hf, Sn, Tb, Zr (Fig 19) and Bi show enrichment in Talet Seliem and Allouga and depletion in Abu Thour and Abu Zarab (F.g19). Pb concentration increases as a result of the presence of Pb minerals such as coronadite and galena. Zr, Hf and Y are relatively immobile and essentially concentrated in the accessory minerals (zircon and its alteration product brannirite, xenotime, thorite and uranothorite). High contents of U, Th, Y, Nb, Ta and REEs may be related to the presence of xenotime Y(HRE) (PO_4), columbite, bastanesite and monazite (Ce, La, Nd, Th) PO_4 as will be indicated from the mineralogical studies (**Bishr, 2012** and the present study).

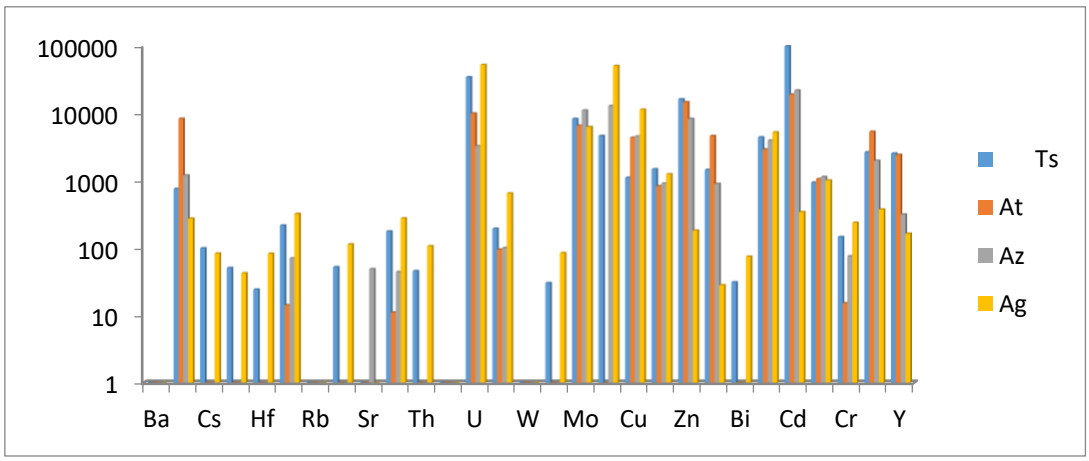

Fig.19: Histogram showing the depletion and enrichment of trace elements of the studied localities.

When the trace elements concentrations of the studied localities correlated with respect to the international shale standard namely; NASC (North American Shale Composite) which is given by **Gromet et al., (1984)** and the Average of stream sediments of Gabal El Hamra area Southern Sinai (No. of samples = 43); **(El Nahas, 2006)**, (Figs. 20, 21,22&23).

It was found that Talet Seliem (Fig. 20) has higher contents of V, Ba, Nb, Zr, Sr, Cu, Pb, Zn, Ni and Cr than NASC and Gabal El Hamra stream. This is mainly attributed to the presence of sulphides (pyrite, chalcopyrite and galena), zircon, carbonate and ferromagnesian minerals.

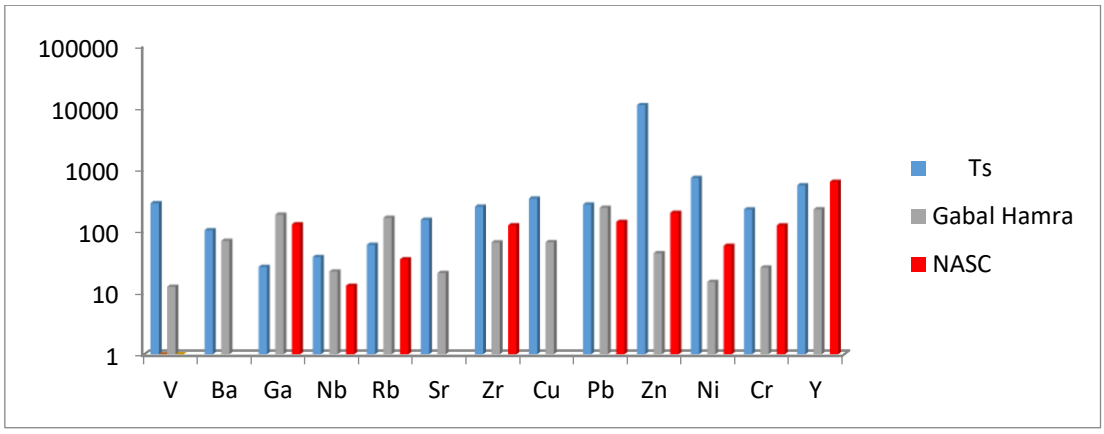

Fig.20: Correlation between trace elements of Talet Seliem and other local and international averages.

In Abu Thour (Fig. 21), it has high contents of V, Sr, Cu, Zn and Ni relative to NASC and Gabal El Hamra sediments. This is mainly related to the presence of sulphides, xenotime, carbonates and ferromagnesian minerals.

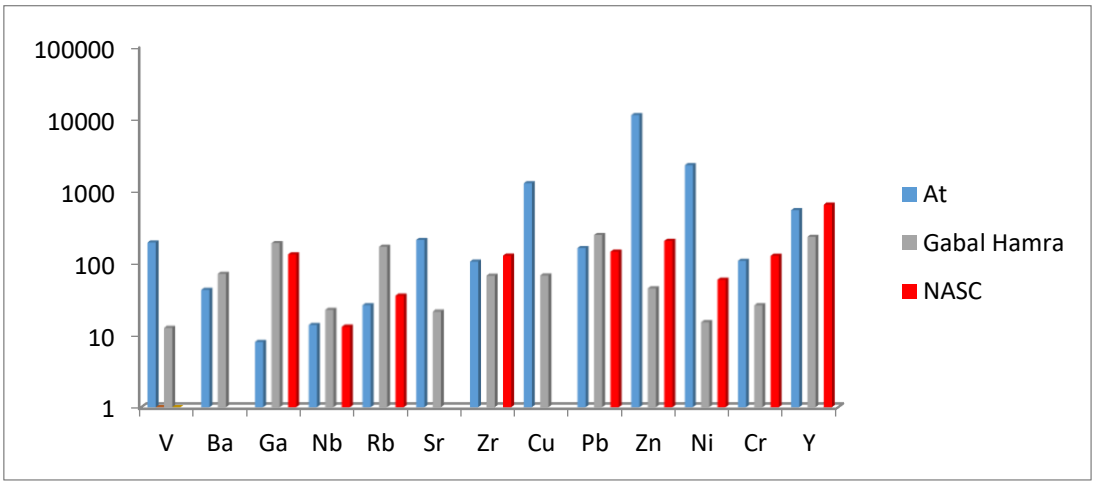

Fig.21: Correlation between trace elements of Abu Thour and other local and international averages.

Allouga (Fig. 22) is enriched in V, Ba, Nb, Sr, Cu, Zn and Cr in correlation with NASC and Gabal El Hamra streams suggesting the presence of slphides and ferromagnesian minerals.

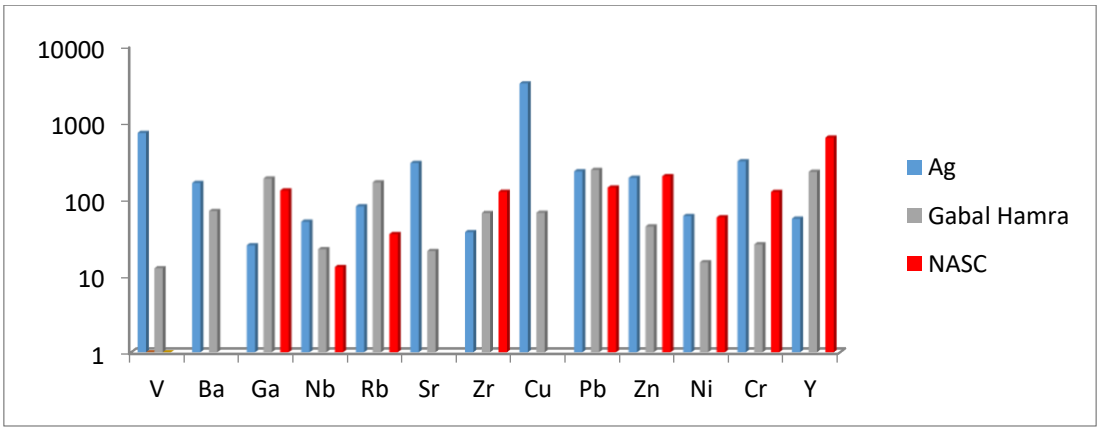

Fig. 22: Correlation between trace elements of Allouga and other local and international averages.

In addition, Abu Zarab locality (Fig. 23) has higher concentrations of V, Ba, Sr, Cu, Zn, Ni and Cr in comparison with NASC and Gabal El Hamra streams indicating the occurrence of barite and ferromagnesian minerals.

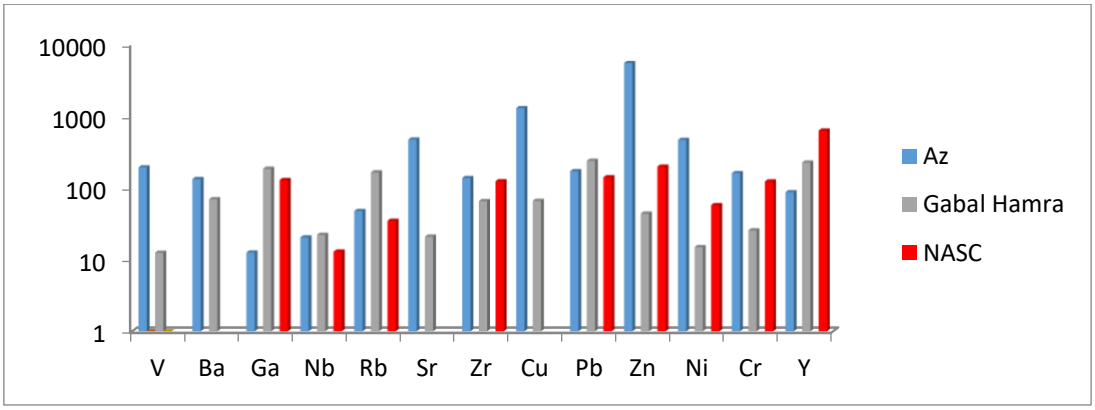

Fig. 23: Correlation between trace elements of Abu Zarab and other local and international averages

It is worthy to mention that marl occur in the middle Um Bogma Formation in the four studied localities. So, the correlation between various elements (major, trace and REEs) must be studied to clarify the behavior of these elements in the media of deposition (Table 4).

Depletion of Rb, Ba, and Cs in the most studied localities could be resulted from the decomposition of feldspars in the source granitic rocks of El Shallal area during alteration processes **(Dawood, 2009)**. The mass gain of Be from the system reflect the essential role of pH changes of mineralizing solutions. **Feng (2011)** showed that low- and high-pH fluids were the principal agent for leaching and fixation of Be in water-rock reaction systems.

The enrichment of Co, Cr and Ni in the studied localities may be related to the presence of ferromagnesian minerals. The strong positive correlation of K with Rb (r = 1.00), Ba (r = 0.88), Ga (r = 0.86), and Cs (r = 0.83) may indicate that Rb, Ba and Cs were fixed by muscovite-illite (Table 4). Also, K shows strong positive correlation with U (r =0.88) and V (r = 0.89) which could be connected with carnotite mineralization as will be shown later. However, it has strong positive correlation with Nb (r = 0.97), Ta (r = 0.96), Z (r = 0.97) and Hf (r = 0.98) which may be mutually substituted in micas.

In addition, it is highly correlated with Tl and Th indicating by the presence of high contents of Tl in jarosite and its participation in thorite composition. High K-Nd correlation (0.87) is clarified by Nd adsorption on clay minerals, iron oxides and gypsum. The strong positive correlation of Fe with Cs (r = 0.70), Ga(r = 0.61), Sr(r = 0.72), Pb(r = 0.80), Cd (r = 0.097), Sb(r = 0.84), Y (r = 0.67), LREEs [La (r = 0.97), Ce(r = 0.99), Pr(r = 0.99), Sm(r = 0.99). Eu(r = 0.99)], moderate correlation with MREEs and HREEs [Dy (r = 0.70), Ho (r = 0.69), Er (r = 0.68), Tm (r = 0.69), Yb (r = 0.71) and Lu (r = 0.69)] and fairly has a positive correlation with Au (r = 0.59), suggesting that these elements may be scavenged by iron oxides which play a significant role in fixation and distribution of these elements.

On the other hand, the strong positive correlation of Ti with Ba (r = 0.71), Co (r = 0.70), Cs (r = 0.89), Ga (r = 0.93), Hf (r = 0.99), Nb (r = 1.00), Rb (r = 0.96), Sn (r = 1.00), Ta (r = 1.00), Th (r = 0.99), Tl (r = 1.00), U (r = 0.97), V (r = 0.89), W (r = 1.00), Zr (r = 1.00), Ag (r = 0.76), Au (r = 0.77), Cu (r = 0.53), Pb (r = 0.80), Ni (r = 0.73), Bi (r = 1.00 As (r = 0.94), Sb (r = 0.64) Cr (r = 0.99), Be (r = 0.79), Li (r = 0.98), Nd (r = 0.76), which indicate that Ti-bearing minerals such as rutile and sphene have been related directly to the distribution of these elements.

The moderate to strong positive correlations of Al with Ba (r = 0.59), Co (r = 0.70), Sr (r = 0.71), Mo (r = 0.75), Zn (r = 0.83), Ni (r = 0.66), Sc (r = 0.94), Lu (r = 0.50)), clarify the enrichment of these elements during kaolinization of these rocks. Silica show strong correlation with Sr (r = 0.97), Mo (r = 0.62), Zn (r = 0.83), Sb (r = 0.93), Li (r = 0.60), Y (r = 0.66), Dy (r = 0.70), Ho (r = 0.69), Er (r = 0.68), Tm (r = 0.69), Yb (r = 0.71), Lu(r = 0.69) indicating the role of clay minerals in redistribution of various elements. All the proceeding correlations clearly show the role of clay minerals, iron oxides and Ti-bearing minerals with the assistance of pH changes and microorganisms in the mobility and fixation of U, REEs, rare metals, gold and silver.

Table 4: Correlation between various elements (major, trace and REEs).

	SiO_2	Al_2O_3	TiO_2	$Fe_2O_3^t$	MgO	CaO	Na_2O	K_2O	MnO	P_2O_5	Ba	Co	Cs	Ga
SiO_2	1.00	0.67	-0.45	-0.70	-0.74	-0.06	0.63	-0.19	0.66	-0.03	0.30	-0.13	-0.72	-0.51
Al_2O_3		1.00	0.01	-0.01	-0.97	-0.69	0.71	0.22	0.05	-0.11	0.59	-0.70	-0.09	0.17
TiO_2			1.00	0.31	0.21	-0.72	-0.64	0.96	-0.94	0.74	0.71	-0.72	0.89	0.93
$Fe_2O_3^t$				1.00	0.05	-0.34	0.03	0.12	-0.60	-0.40	-0.16	-0.24	0.70	0.61

MgO					1.00	0.52	-0.85	0.01	-0.26	0.30	-0.40	0.53	0.27	0.04
CaO						1.00	-0.07	-0.81	0.68	-0.36	-0.86	0.99	-0.63	-0.82
Na_2O							1.00	-0.51	0.57	-0.73	-0.13	-0.05	-0.53	-0.40
K_2O								1.00	-0.84	0.80	0.88	-0.83	0.76	0.86
MnO									1.00	-0.49	-0.51	0.64	-0.99	-0.98
P_2O_5										1.00	0.71	-0.42	0.38	0.44
Ba											1.00	-0.90	0.41	0.62
Co												1.00	-0.59	-0.78
Cs													1.00	0.96
Ga														1.00

Table 4: Cont.

	Hf	Nb	Rb	Sn	Sr	Ta	Th	Tl	U	V	W	Zr	Mo	Ag	Au
SiO_2	-0.38	-0.42	-0.18	-0.39	0.97	-0.45	-0.34	-0.45	-0.62	-0.27	-0.41	-0.42	0.75	0.01	-0.91
Al_2O_3	0.02	0.05	0.27	0.04	0.71	-0.01	0.06	0.01	-0.23	-0.17	0.00	0.00	0.91	-0.02	-0.51
TiO_2	0.99	1.00	0.96	1.00	-0.22	1.00	0.99	1.00	0.97	0.89	1.00	1.00	-0.39	0.76	0.77
Fe_2O_3 t	0.21	0.30	0.17	0.25	-0.72	0.29	0.19	0.31	0.33	-0.13	0.23	0.24	-0.06	-0.39	0.59
MgO	0.21	0.18	-0.04	0.19	-0.72	0.23	0.17	0.21	0.44	0.38	0.23	0.23	-0.98	0.22	0.66
CaO	-0.70	-0.74	-0.85	-0.73	-0.24	-0.70	-0.73	-0.72	-0.53	-0.46	-0.70	-0.70	-0.36	-0.43	-0.24
Na_2O	-0.66	-0.62	-0.46	-0.63	0.49	-0.66	-0.63	-0.64	-0.79	-0.81	-0.67	-0.67	0.93	-0.68	-0.78
K_2O	0.98	0.97	1.00	0.98	0.06	0.96	0.99	0.96	0.88	0.89	0.97	0.97	-0.20	0.84	0.56
MnO	-0.91	-0.94	-0.85	-0.92	0.47	-0.94	-0.89	-0.94	-0.94	-0.71	-0.91	-0.92	0.40	-0.51	-0.88
P_2O_5	0.80	0.74	0.76	0.77	0.19	0.75	0.81	0.74	0.73	0.96	0.79	0.78	-0.45	1.00	0.39
Ba	0.75	0.74	0.88	0.75	0.52	0.71	0.78	0.71	0.54	0.69	0.74	0.73	0.23	0.77	0.10
Co	-0.71	-0.74	-0.86	-0.74	-0.31	-0.70	-0.74	-0.72	-0.53	-0.50	-0.71	-0.71	-0.36	-0.50	-0.20
Cs	0.84	0.89	0.77	0.86	-0.56	0.89	0.83	0.89	0.90	0.62	0.85	0.86	-0.40	0.39	0.90
Ga	0.89	0.93	0.88	0.91	-0.33	0.92	0.88	0.93	0.87	0.65	0.89	0.90	-0.19	0.47	0.76
Hf	1.00	0.99	0.97	1.00	-0.15	1.00	1.00	0.99	0.96	0.93	1.00	1.00	-0.39	0.82	0.72
Nb		1.00	0.97	1.00	-0.19	1.00	0.99	1.00	0.96	0.88	1.00	1.00	-0.35	0.76	0.75
Rb			1.00	0.97	0.06	0.95	0.98	0.96	0.86	0.86	0.96	0.96	-0.14	0.80	0.55
Sn				1.00	-0.16	1.00	1.00	1.00	0.96	0.91	1.00	1.00	-0.36	0.80	0.73
Sr					1.00	-0.22	-0.10	-0.22	-0.40	-0.04	-0.17	-0.18	0.69	0.24	-0.79
Ta						1.00	0.99	1.00	0.97	0.90	1.00	1.00	-0.41	0.77	0.77
Th							1.00	0.99	0.95	0.92	1.00	1.00	-0.35	0.83	0.69
Tl								1.00	0.97	0.89	1.00	1.00	-0.39	0.76	0.77
U									1.00	0.89	0.97	0.97	-0.60	0.73	0.88
V										1.00	0.92	0.92	-0.54	0.96	0.62
W											1.00	1.00	-0.40	0.81	0.74

Zr												1.00	-0.40	0.80	0.75
Mo													1.00	-0.37	-0.75
Ag														1.00	0.36
Au															1.00

Table 4: Cont.

	Cu	Pb	Zn	Ni	Bi	As	Cd	Sb	Cr	Be	Sc	Li	In	Re	Y
SiO_2	0.11	-0.63	0.96	-0.23	-0.51	-0.15	-0.52	0.93	-0.30	-0.19	0.42	0.60	0.58	-0.16	-0.66
Al_2O_3	-0.18	0.12	0.83	-0.66	-0.07	0.32	0.17	0.36	0.13	-0.53	0.94	0.18	0.99	-0.19	-0.50
TiO_2	0.53	0.80	-0.43	-0.73	1.00	0.94	0.15	-0.64	0.99	-0.79	0.34	-0.98	0.02	0.80	-0.32
Fe_2O_3 t	-0.62	0.80	-0.47	-0.02	0.32	0.17	0.97	-0.84	0.19	0.08	0.18	-0.35	0.12	-0.29	0.67
MgO	0.33	0.05	-0.90	0.47	0.29	-0.09	-0.16	-0.47	0.10	0.33	-0.84	-0.40	-0.97	0.38	0.39
CaO	-0.14	-0.73	-0.22	0.94	-0.66	-0.87	-0.35	0.30	-0.77	0.88	-0.90	0.58	-0.71	-0.36	0.46
Na_2O	-0.69	-0.29	0.80	0.06	-0.70	-0.42	0.27	0.51	-0.58	0.21	0.48	0.76	0.74	-0.80	0.05
K_2O	0.62	0.69	-0.18	-0.88	0.94	0.99	0.00	-0.42	0.99	-0.92	0.50	-0.90	0.20	0.83	-0.56
MnO	-0.25	-0.94	0.57	0.58	-0.95	-0.83	-0.44	0.85	-0.88	0.60	-0.29	0.95	0.00	-0.58	0.01
P_2O_5	0.96	0.19	-0.20	-0.60	0.74	0.74	-0.56	-0.07	0.79	-0.74	0.08	-0.72	-0.19	0.99	-0.71
Ba	0.59	0.41	0.31	-0.98	0.66	0.90	-0.18	0.01	0.82	-0.99	0.75	-0.57	0.54	0.67	-0.83
Co	-0.22	-0.67	-0.26	0.97	-0.66	-0.89	-0.26	0.23	-0.79	0.92	-0.90	0.57	-0.71	-0.41	0.55
Cs	0.13	0.97	-0.61	-0.50	0.90	0.76	0.54	-0.91	0.82	-0.51	0.26	-0.91	-0.02	0.48	0.12
Ga	0.17	0.96	-0.39	-0.71	0.91	0.88	0.50	-0.77	0.89	-0.69	0.49	-0.89	0.22	0.51	-0.10
Hf	0.61	0.74	-0.39	-0.75	0.99	0.95	0.05	-0.57	0.99	-0.82	0.34	-0.97	0.01	0.85	-0.41
Nb	0.53	0.81	-0.40	-0.76	0.99	0.96	0.15	-0.63	0.99	-0.81	0.38	-0.97	0.06	0.79	-0.34
Rb	0.56	0.72	-0.15	-0.90	0.93	1.00	0.06	-0.44	0.99	-0.93	0.56	-0.88	0.26	0.78	-0.54
Sn	0.57	0.77	-0.38	-0.76	0.99	0.96	0.09	-0.59	0.99	-0.82	0.36	-0.97	0.04	0.82	-0.39
Sr	0.30	-0.49	0.91	-0.44	-0.28	0.09	-0.56	0.85	-0.05	-0.42	0.53	0.38	0.61	0.06	-0.82
Ta	0.55	0.79	-0.44	-0.73	1.00	0.94	0.12	-0.64	0.99	-0.78	0.32	-0.98	0.00	0.81	-0.33
Th	0.62	0.73	-0.35	-0.78	0.98	0.97	0.03	-0.54	1.00	-0.85	0.37	-0.96	0.05	0.85	-0.44
Tl	0.53	0.80	-0.43	-0.73	1.00	0.94	0.15	-0.64	0.99	-0.79	0.34	-0.98	0.02	0.80	-0.32
U	0.54	0.77	-0.63	-0.55	0.99	0.84	0.13	-0.73	0.92	-0.63	0.11	-1.00	-0.22	0.81	-0.17
V	0.86	0.45	-0.39	-0.62	0.89	0.84	-0.31	-0.35	0.90	-0.75	0.10	-0.89	-0.22	0.99	-0.54
W	0.60	0.75	-0.41	-0.74	0.99	0.95	0.06	-0.59	0.99	-0.81	0.32	-0.98	0.00	0.84	-0.38
Zr	0.59	0.76	-0.42	-0.74	0.99	0.95	0.08	-0.60	0.99	-0.80	0.32	-0.98	0.00	0.84	-0.37
Mo	-0.44	-0.17	0.91	-0.30	-0.46	-0.09	0.17	0.53	-0.28	-0.15	0.73	0.55	0.91	-0.53	-0.27
Ag	0.95	0.23	-0.14	-0.67	0.75	0.79	-0.53	-0.06	0.82	-0.79	0.16	-0.72	-0.11	0.98	-0.75
Au	0.20	0.78	-0.89	-0.15	0.81	0.52	0.38	-0.93	0.65	-0.21	-0.19	-0.87	-0.45	0.51	0.31
Cu	1.00	-0.08	-0.11	-0.44	0.53	0.55	-0.76	0.14	0.60	-0.59	-0.08	-0.52	-0.29	0.93	-0.74

Pb		**1.00**	**-0.46**	**-0.54**	**0.80**	**0.72**	**0.71**	**-0.87**	**0.74**	**-0.50**	**0.43**	**-0.79**	**0.20**	**0.29**	**0.16**
Zn			**1.00**	**-0.29**	**-0.50**	**-0.11**	**-0.25**	**0.81**	**-0.29**	**-0.21**	**0.60**	**0.60**	**0.77**	**-0.32**	**-0.55**
Ni				**1.00**	**-0.68**	**-0.92**	**-0.02**	**0.10**	**-0.82**	**0.98**	**-0.84**	**0.59**	**-0.63**	**-0.57**	**0.73**
Bi					**1.00**	**0.92**	**0.14**	**-0.68**	**0.97**	**-0.74**	**0.27**	**-0.99**	**-0.06**	**0.80**	**-0.27**
As						**1.00**	**0.07**	**-0.41**	**0.98**	**-0.94**	**0.60**	**-0.86**	**0.30**	**0.76**	**-0.56**
Cd							**1.00**	**-0.69**	**0.05**	**0.12**	**0.30**	**-0.15**	**0.30**	**-0.47**	**0.65**
Sb								**1.00**	**-0.51**	**0.10**	**0.06**	**0.73**	**0.26**	**-0.20**	**-0.51**
Cr									**1.00**	**-0.88**	**0.44**	**-0.94**	**0.12**	**0.83**	**-0.47**
Be										**1.00**	**-0.72**	**0.66**	**-0.49**	**-0.71**	**0.78**
Sc											**1.00**	**-0.16**	**0.95**	**0.03**	**-0.50**
Li												**1.00**	**0.16**	**-0.79**	**0.18**
In													**1.00**	**-0.26**	**-0.39**
Re														**1.00**	**-0.62**
Y															**1.00**

V. Conclusions

The marl unit of the middle member of Um Bogma Formation has wide exposure and highest thickness and radioactivity. So, four localities were chosen for detailed radiometrical, mineralogical and geochemical and studies: Talet Seliem, Abu Thor, Allouga and Abu Zarab.

The eU/eTh values of the investigated marl suggesting that these rocks are considered as productive uraniferous rocks and sites of deposition, especially at Talet Seliem and Allouga. The lesser values of chemically measured uranium with respect to radiometrically measured indicate uranium migration from the marl to the other rock types in the same formation or other formations (migration out). One sample in Talet Seliem and other one in Allouga show highvalues of chemically measured uranium with respect to radiometrically measured indicate uranium migration from the other rock types in the same formation or other formations to the marl (migration in).

Mineralogical studies of the Talet Seliem, Abu Thour, Allouga and Abu Zarab localities clarified that the mineral association are mainly represented by autonite, cerianite, pyrite, corandite, iron oxides and clays-bearing REEs and bastanesite in Talet Seliem REEs mainly Nd adsorbed on clay and gypsum, aurorite and monazite in Abu Thour, brannerite, uraninite, carnotite and torbernite in Allouga and thorite, paratacamite, malachite, galena and jarosite in Abu Zarab, also gold is present in the four localities.

Geochemical studies indicated that the marl of Talet Seliem, Abu Thour, Allouga and Abu Zarab localities is highly enriched in Ag, Au, U and REEs, in addition to Zn, Cu and Pb. Gold and silver are present in the four localities with anomalous contents reaches 1.78 and 27.15 ppm respectively.

The REE patterns of the studies rocks are characterized by successive enrichment in REE contents from Talet Seliemto Allouga, Allouga has the highest uranium contents. REEs showed that the marl was subjected to severe physic-chemical changes as induced from the unusual values of isovalents and REEs tetrad effect.

It can be concluded that U and REEs were likely leached from the upper acidic environments (Talet Seliem, Abu Thor and Abu Zarab) and concentrated in the lower alkalic zone under reducing conditions (Allouga) as indicated from geomorphological studies.Correlations coefficient between major oxides, trace and REEs clearly show the role of clay minerals, iron oxides and Ti-bearing minerals with the assistance of pH changes and microorganisms in the mobility and fixation of U, REEs, and rare metals, gold and silver.

References

[1]. **Alshami, A.S. (2017)**: U-minerals and REE distribution, paragenesis and provenance of Um Bogma Formations, southwestern Sinai, Egypt. Nuclear Sciences Scientific Journal.

[2]. **Alshami, A.S. (2018):**Infra-Cambriand placer gold-uraniferous Paleozoic sediments, southwestern Sinai, Egypt. Nuclear Sciences Scientific Journal.

[3]. **Abedini, A., RezaeiAzizi, M., Calagari, A.A., Cheshmehsari, M. (2017):**Rare earth element geochemistry and tetrad effects of the Dalirphosphaticshales, northern Iran. N. J. Geol. Paläont. Abh.286, pp.169–188.

[4]. **Abedini, A., Calagarib, A. A., Azizia,M. R. (2018):**The tetrad-effect in rare earth elements distribution patterns of titanium-rich bauxites: Evidence from the Kanigorgeh deposit, NW IranJournal of Geochemical Exploration 186, pp.129–142.

[5]. **Anders, E. and Grevesse, N. (1989):** Abundances of the elements: Meteoritic and solar Geochim. Comochim.Acta 53, pp.197-214.

[6]. **Auer, G., Reuter, M., Hauzenberger, C.A. &Piller, W.E.(2017):** The impact of transport processes on rare earth element patterns in marine authigenic and biogenic phosphates. – GeochimicaetCosmochimicaActa, 203: pp.140-156.

[7]. **Barron, T.(1907):**The Topography and Geology of the Peninsula of Sinai (Western portion). Egyptian Survey Department, Cairo. 241p.

[8]. **Bau, M. and Dulski, P. (1995):** Comparative study of yttrium and rare-earth element behaviours in fluorine-rich hydrothermal fluids. Contrib. Mineral. Petrol. 119: pp. 213-223.

[9]. **Bau, M. (1996):** Controls on the fractionation of isovalent trace elements in magmatic and aqueous systems: evidence from Y/Ho, Zr/Hf and lanthanide tetrad effect. Contrib. Mineral. Petrol., 123: pp.323-333.

[10]. **Bau, M. (1999):** Scavenging of dissolved yttrium and rare earths by precipitating iron oxyhydroxide: Experimental evidence for Ce oxidation, Y-Ho fractionation, and lanthanide tetrad effect. Geochim.Cosmochim.Acta, 63: pp.67-77.

[11]. **Bishr, A. H. (2012):**Primary uranium mineralization in paleochannels of the Um Bogma Formation at Allouga, Southwestern Sinai, Egypt.Eleventh Arab Conference on the Peaceful Uses of Atomic Energy. Khartoum. Sudan. pp.16-20.

[12]. **Crinci, J., Jurkowic, I. (1990):**Rare earth elements in Triassic bauxites of Croatia

[13]. Yugoslavia. In: Travaux. 19. pp.239–248.

[14]. **Darnely, A. G. (1982):** "Hot granite"; some general remarks. In: Uranium in granites (ed), Y.T. Maurice: Geological Survey of Canada, pp. 81-23, 1-10

[15]. **Dawood, Y. H.(2009):**Radiogenic Isotope Fractionation as an Indication for Uranium Mobility in the Granites of El Shallal Area, West Central Sinai, Egypt.JKAU; Earth Sci., 20, 1, pp.215-238.

[16]. **El Aassy, I.E.; Botros, N.H.; Abdel Razik, A;Alshami, A.S.; Ibrahim, S.K.; Sherif, H.Y.; Attia, K.E., and Moufei, A.A(1986):**Report on proving of some radioactive occurrences in west central Sinai. Int. Rept. N.M.A., CairoEgypt.

[17]. **El Nahas, H. A.; Desouky, O. A.; Abdel Monsif, M.; El Sayed, N. S.(2016):** Stream Sediments Survey for Uranium in Wadi El-Reddah, North Eastern Desert, Egypt. Al Azhar J. Science.

[18]. **El Shazly, E.M.; El Hazak, N.M.; Abdel Monem,A.A.; Khawasik, S.M.; Zayed, Z.M.; Mostafa, M.E., and Morsi, M.A.(1974)**: Origin of uranium of Oligocene Qatrani sediments, Western Desert, Egypt. I.A.E.A. , Vienna.

[19]. **El Sokkary, A.A. (19630**: Geologic and mineralogical studies of some radioactive deposits in west central Sinai. M. Sc. Thesis, Fac. Sci., Alexandria univ., 132 p.

[20]. **Flinter, B.H. (1959):** A magnetic separation of some alluvial minerals in Malaya. American.Mineralogist, V. 44, No. 7-8, pp.738-751.

[21]. **Feng, J.L., Gao, S.P., Zhang, J.F. (2011):**Lanthanide tetrad effect in ferromanganese concretions and terra rossa overlying dolomite during weathering. Chem. Erde 71, pp.349–362.

[22]. **Fernández-Caliani, J.C., Galán, E., Aparicio, P., Miras, A.,Márquez, and M.G. (2010):**Origin and geochemical evolution of the Nuevo Montecastelo kaolin deposit (Galicia, NW Spain). Applied Clay Science, 49: pp.91–97.

[23]. **Gromet, L. P., Dymek, R. F., Haskin, L. A. and Korotev, R. L. (1984):** The North American shale composite—its compilation, major and trace element characteristics. Geochim.Cosmochim.Acta, 48, pp.2469–2482.

[24]. **Irber, W. (1999):** The lanthanide tetrad effect and its correlation with K/Rb, Eu/Eu*, Sr/Eu, Y/Ho, and Zr/Hf of evolvingperaluminous granite suites. Geochim.Cosmochim.Acta.63, pp.489–508.

[25]. **Issawi, B., and Jux,U. (198):**Contribution to the stratigraphy of the Paleozoic rocks in Egypt. Geol. Surv. , No.64, 28p.

[26]. **Jahn, B., Wu, F., Capdevila, R., Martineau, F., Zhao, Z. and Wang, Y. (2001):** highly evolved juvenile granites with tetrad REE patterns: the Woduhe and Baerzhe granites from the Great Xing'an Mountains in NE China. Lithos. 59: pp.171-198.

[27]. **Koppi A.J, Edis R, Foeld D.J, Geering H.R, Klessa D.A, Cockayne D.J.H. (1996):**REEs trends and Ce-U-Mn associations in weathered rock from Koongarra, northern territory, Australia. GeochimCosmochim Ac 60: pp.1695–1707.

[28]. **Kora, M.(1984:** The Paleozoic outcrops of Um Bogma area, Sinai. Ph.D. Thesis, Mansoura Univ., Egypt, 280p.

[29]. **Maksimovic, Z., Pantó, G.(1996):**Authigenic rare earth minerals in karst-bauxites andkarstic nickel deposits. In: Jones, F.A., Wall, F., Williams, C.T. (Eds.), Rare Earth Minerals, Chemistry, Origin and Ore Deposits, First Edition. Springer Science and Business Media,pp.257–259.

[30]. **Mclennan, s.m. (1994):** Rare earth element geochemistryand the "tetrad" effect. – GeochimicaetCosmochimicaActa, 58: pp. 2025-2033.

[31]. **Monecke, T., Dulski, P. &Kempe, U. (2007):** Origin of convex tetrads in rare earth element patterns of hydrothermally altered siliceous igneous rocks from the ZinnwaldSn–W deposit, Germany. – GeochimicaetCosmochimicaActa, 71: pp.335-353.

[32]. **Nardi, L.V.S., Formoso, M.L.L., Jarvis, K., Oliveira, l.,BastosNeto, A.C. & Fontana, e. (2012):** REE, Y, Nb, U, and Th contents and tetrad effect in zircon from a magmatic-hydrothermal F-rich system of Sn-rare metalecryolite mineralized granites from the Pitinga Mine, Amazonia, Brazil. – Journal of South American Earth Sciences, 33: pp.34-42.

[33]. **Naumov, G.B. (1959):** Transportation of uranium in hydrothermal solution as carbonate Geochemistry, V.1, pp. 5-20

[34]. **Omara, S., and Conil, R.(1956):** Lower Carboniferous foraminifera from southwestern Sinai, Egypt. Annals Soc. Geol. Belgique, 88, pp.221-240.

[35]. **Pan, Y. (1997):** Controls on the fractionation of isovalent trace elements in magmatic and aqueous systems: evidence from Y/Ho, Zr/Hf, and lanthanide tetrad effect- a discussion of the article by M. Bau (1996), Contrib. Mineral. Petrol. 128: pp.405-408.

[36]. **Rogers J.J.W. and Adams J.A.S. (1969)** Uranium and thorium.InHandbook of Geochemistry (ed. Wedepohl K.H.) [M]. VII-3, 92-B-1 to 92-0-8and 90-B-1 to 90-0-5, Springer Verlag, Berlin.

[37]. **Rudnick, R. L. and Gao, S. (2004):** Composition of the Continental Crust. In: Treatise on Geochemistry. Holland, H.D. and Turekian, K.K. (Editors), Elsevier, Amsterdam. 3: pp.1-64.

[38]. **Soliman, S.M., and Fetouh, M.(1969)**: Petrology of the Carboniferous sandstone in West Central Sinai. J. Geol.U.A.R.13/2, 61-143.

[39]. **Taylor, S. R. and McLennan, S. M. (1985):**The Continental Crust; Its composition and evolution; an examination of the geochemical record preserved in sedimentary rocks. Blackwell, Oxford, 312p.

[40]. **Weissbroad, T.(1969)**: Paleozoic outcrops in south Sinai and their correlation with those of southern Palestine. In: The Paleozoic of Israel and adjacent countries. Bull. Geol. Surv., 17(2), 32p.